Effects of tunneling on groundwater flow and swelling of clay-sulfate rocks

Citation: Butscher, Christoph, Herbert H. Einstein, and Peter Huggenberger. "Effects of Tunneling on Groundwater Flow and Swelling of Clay-sulfate Rocks." Water Resources Research 47.11 (2011).

As Published: http://dx.doi.org/10.1029/2011wr011023

Publisher: American Geophysical Union (AGU)

Persistent URL: http://hdl.handle.net/1721.1/77636

Version: Author's final manuscript: final author's manuscript post peer review, without publisher's formatting or copy editing

Effects of tunneling on groundwater flow and swelling of clay-sulfate rocks

Christoph Butscher[1], Herbert H. Einstein[1], Peter Huggenberger[2]

[1] Massachusetts Institute of Technology, Department of Civil and Environmental Engineering, 77 Massachusetts Avenue, Cambridge, MA 02139, USA

[2] University of Basel, Institute of Geology and Paleontology, Applied and Environmental Geology, Bernoullistrasse 32, 4056 Basel, Switzerland

Corresponding author: Christoph Butscher, e-mail: butscher@mit.edu, phone: +1 617 715 4766, fax: +1 617 253 6044

Abstract

Swelling of clay-sulfate rocks is a major threat in tunneling. It is triggered by the transformation of the sulfate mineral anhydrite into gypsum as a result of water inflow in anhydrite-containing layers after tunnel excavation. The present study investigates the hydraulic effects of tunneling on groundwater flow and analyzes how hydraulic changes caused by excavation lead to water inflow into anhydrite-containing layers in the tunnel area. Numerical groundwater models are used to conduct scenario simulations that allow one to relate hydrogeological conditions to rock swelling. The influence of the topographic setting, the excavation damaged zone around the tunnel, the sealing effect of the tunnel liner and the geological configuration are analyzed separately. The analysis is performed for synthetic situations and is complemented by a case study from a tunnel in Switzerland. The results illustrate the importance of geological and hydraulic information when assessing the risk of swelling at an actual site.

Keywords: groundwater flow; groundwater modeling; rock swelling; clay-sulfate rocks; tunneling

1. Introduction

Tunneling in clay-sulfate rocks often faces substantial engineering problems because of the swelling behavior of such rock [*Einstein*, 1996; *Anagnostou et al.*, 2010]. The swelling manifests itself by heave of the tunnel floor, destruction of the lining or even uplift of the entire tunnel and the ground surface above [e.g., *Anagnostou*, 1992]. Rehabilitation of damaged tunnels causes disruption of major transportation links and produces high additional costs. Examples of tunnels that are affected by swelling clay-sulfate rocks include tunnels crossing the Triassic Gipskeuper ("Gypsum Keuper") formation in the Jura Mountains of Switzerland and France, and in the Stuttgart metropolitan area in Germany [*Steiner*, 1993]. Engineering problems related to the swelling of clay-sulfate rocks are also reported from other countries, including Spain [*Alonso and Olivella*, 2008], Saudi Arabia [*Azam*, 2007], Poland, Italy and Texas/USA [*Yilmaz*, 2001, and references therein]. It is likely, although not known by the authors, that more cases exist elsewhere. The problems associated with the swelling are likely to gain even more relevance in the near future. In the area of Stuttgart, for example, a major railway project (Stuttgart 21 [*Wittke*, 2007]) is currently planned that involves many additional kilometers of underground infrastructure within the Gipskeuper.

The threat of swelling is mostly counteracted on an engineering level by constructive measures. Countermeasures are planned based on the relation between swelling deformation and swelling pressure. In pure clay rocks, for example, there is a linear relation between swelling heave and the logarithm of pressure [*Madsen and Vonmoos*, 1989]. In clay rocks containing sulfate minerals, however, an accepted relation describing the heave as a function of pressure is still lacking. In practice, engineers face the problem that swelling heave and pressure are hardly predictable during project planning. Field and laboratory experiments often give contradictory indications [*Nüesch et al.*, 1995], and thermodynamic calculations of crystallization pressures [*Ping and Beaudoin*, 1992] are not supported by experimental data [*Flückiger et al.*, 1994]. Major problems in swelling experiments arise from the fact that such experiments last extremely long [*Pimentel*, 2007a, 2007b]. Some of them have been run for more than 20 years without reaching final (equilibrium) conditions. In addition, field-scale conditions controlling the swelling process (actual permeabilities, pore water pressures, geochemistry) are rarely known accurately, and therefore difficult to represent in the laboratory.

The basic mechanism that causes the swelling of clay-sulfate rocks is the transformation of the water-free calcium-sulfate anhydrite ($CaSO_4$) into its water-containing modification gypsum ($CaSO_4 \cdot 2H_2O$) [e.g., *Blount and Dickson*, 1973]. This reaction entails a ~60% volume increase of the transformed sulfate minerals. In a closed system (without water inflow), the volume of gypsum is ~10% less than that of its educts anhydrite plus water, and an increase in total rock volume cannot be expected. In a system open to water inflow, however, the total rock volume increases when anhydrite transforms in to gypsum, provided that the increase in volume of the sulfate minerals is not compensated by a decrease in pore water volume. Changes in pore water volumes can occur by anhydrite solution and gypsum precipitation during the swelling process. However, differences in pore water volume of clay rocks containing anhydrite and clay rocks containing gypsum are considered to be minor, and small changes in pore water volume lead to even smaller changes in total rock volume. From this consideration it follows that observed swelling of clay-sulfate rocks (i.e., an increase in total rock volume) requires both water uptake by anhydrite to form gypsum, and, concurrently, water inflow. Figure 1 shows a volume balance of the transformation of anhydrite into gypsum for clay-sulfate rocks in an open system, assuming a constant pore water volume.

[Figure 1 near here]

Given that water inflow into clay-sulfate rocks is a prerequisite for swelling, groundwater flow is likely to be a major controlling factor of the swelling process. Despite its importance, hydrogeological aspects have attracted little attention in the investigation of swelling processes so far [*Hauber et al.*, 2005]. *Butscher et al.* [2011a] investigated the effects of regional groundwater flow on swelling clay-sulfate rock in tunneling. They concluded that tunnel excavation causes an increase of flow rates around the tunnel and changes the capture zone of the tunnel and geochemical conditions in the tunnel zone. They also presented a case study that investigated the hydraulic changes induced by tunneling in the Chienberg tunnel (Switzerland), and related these changes to the swelling in different zones of

the tunnel [*Butscher et al.*, 2011b]. The findings suggest that in certain situations the tunnel and its surrounding excavation damaged zone provide pathways for groundwater flow from water-containing units above the tunnel to anhydritic layers at the tunnel invert. The resulting groundwater inflow into anhydritic layers probably triggers the transformation of anhydrite into gypsum and, thus, causes rock swelling.

So far, there are two major limitations in the studies that investigated the influence of groundwater flow on the swelling of clay-sulfate rocks. The first concerns model uncertainties in the case studies. Typically, hydraulic properties of the geological units, the tunnel liner and its surrounding excavation damaged zone are not well known in tunneling projects. Also the hydraulic potential and its change due to excavation are rarely measured. The second limitation of the studies so far is that they were conducted in a specific hydrogeological situation. The effects of different hydrogeological conditions on the swelling potential of clay-sulfate rocks, however, have not been systematically investigated so far. To overcome these limitations, another approach was chosen in the present study. The effects of tunneling on the flow field have been investigated by scenario simulations in synthetic situations. The scenarios are designed to represent different geological and hydrological situations as well as different properties of natural and engineered structures that influence water inflow into anhydrite-bearing strata. This allows us to separately analyze the impact of different factors on the swelling of clay-sulfate rocks.

2. Conceptual approach

2.1 Basic concept

The basic assumption underlying this study is that groundwater flow rates in aquitards (e.g., k = 1E-10 ms^{-1}) are insufficient to transform anhydrite into gypsum and cause rock swelling. We assume that this transformation and thus swelling only take place when water from an aquifer (e.g., k = 1E-6 ms^{-1}) reaches anhydrite-bearing layers. Therefore, we analyzed water inflow into these layers through numerical groundwater modeling. We used the finite element code FEFLOW [*Diersch*, 2009a] to simulate steady-state saturated groundwater flow. In this paper, we first introduce a "reference model" and show how hydraulic conditions are changed by tunneling, and how these changes can lead to water inflow into anhydrite-bearing layers. Then, scenarios are presented to illustrate how different factors control hydraulic conditions and water inflow into these layers. The factors we consider are:

1. Topographic position of tunnel and resulting "superimposed" flow conditions;
2. Sealing ("tightness") of the tunnel, i.e., the ability of the tunnel to prevent water inflow into the tunnel;
3. Excavation damaged zone (EDZ) around the tunnel;
4. Geological setting, including the spatial configuration of aquifers and aquitards, the position of the anhydrite level (AL) relative to the tunnel, and preferential pathways for groundwater flow provided by faults.

2.2 Topographic position of tunnel

The topography has a strong influence on developing groundwater flow patterns [*Hubbert*, 1940]. In

homogeneous ground, the groundwater table is strongly related to the topography, i.e., it approximately follows the ground surface. Relevant parameters are the relief (topographic highs and lows) and the slope (horizontal distance between highs and lows) [*Tóth*, 1962, 1963]. The hierarchical nature of the topography leads to a hierarchical pattern of flow systems [*Zijl*, 1999]: Generally, regional, intermediate and local flow systems can be distinguished. The position of a tunnel relative to these flow systems is expected to be an important, controlling factor for swelling of clay-sulfate rocks.

The concept of topography-driven flow systems predicts descending flow systems below topographic highs, and ascending flow systems below topographic lows. A simple groundwater model illustrates this concept (Figure 2). In this simple model, the ground surface is a specified head boundary (1st kind boundary condition, Dirichlet type) where the hydraulic head corresponds to the elevation of the ground surface (i.e., the water table is approximated by the ground surface). All other model boundaries are no-flow boundaries. The hydraulic properties of the subsurface are homogeneous and isotropic. The resulting hydraulic gradient in this model is downward near the hill, upward near the valley and basically horizontal in between. In our scenario simulations, we will account for the topographic position of the tunnel by superimposing downward ("hill position"), upward ("valley position") and horizontal ("slope position") gradients to our model domain using appropriate boundary conditions.

[Figure 2 near here]

2.3 Sealing of tunnel

In the saturated zone, tunnels are acting as drains. The drainage effect of a tunnel strongly depends on its "sealing" properties. While a tight tunnel is affecting subsurface hydraulics only to a minor degree, large outflows of groundwater into the tunnel have major effects on flow around the tunnel. The sealing of a tunnel is determined by the material and thickness of the tunnel liner. Sealing can be increased by the placement of polymeric membranes [e.g., *Caputo and Huez*, 1987] or grouting [e.g., *Butrón et al.*, 2010] behind the tunnel lining.

2.4 Excavation damaged zone (EDZ)

An EDZ is expected to exist around tunnels [*Tsang et al.*, 2005]. This zone is characterized by increased fracturing, induced by the excavation and stress redistribution. The induced fractures lead to a considerable increase in rock permeability and provide the possibility for preferential flow. *Tsang et al.* [2005] reported an increase in hydraulic conductivity of up to 6 orders of magnitude and an extent of one tunnel radius outside the tunnel perimeter for that zone within indurated clays. These estimates are based on tests at Mont Terri (Switzerland) and Tournemire (France) underground laboratories. However, the properties of the EDZ will depend on many conditions, among others on the initial stress field, the material properties (e.g., material anisotropy), the existence of natural fracture zones or local inhomogeneities of the rock mass and the geometry of the tunnel [*Blümling et al.*, 2007]. Also the excavation method (e.g., blasting, tunnel boring machine) plays an important role [*Sato et al.*,

2000].

2.5 Geological setting

The geometrical configuration of geological units with different hydraulic properties, e.g., a layering of aquifers and aquitards, is an important aspect to consider if flow systems are to be determined. Faults may further modify the geological configuration, as they may contain highly fractured zones that act as preferential pathways for groundwater flow [*Caine et al.*, 1996]. Faults can therefore strongly modify hydraulic conditions [*Freeze and Witherspoon*, 1967]. The position of a tunnel relative to geological units and faults is therefore expected to have large impact on water inflow into tunnels, as will also become evident later in this paper.

In clay-sulfate rocks, a "gypsum level" (GL) and an "anhydrite level" (AL) can often be observed [e.g., *Noher et al.*, 2010; *Steiner*, 1993; *Murray*, 1964]. The GL separates the zone where sulfate minerals are present in the form of gypsum from a zone where all sulfate minerals are leached. In the leached zone, which is usually closer to the ground surface, a gypsum karst may have developed. The leached zone often corresponds to the weathered zone of the clay-sulfate rocks. It may contain considerable amounts of groundwater and have higher hydraulic conductivities than the non-leached/non-weathered zone, and can be considered to be an aquifer. The spatial configuration of the GL is therefore expected to influence flow patterns.

The AL separates the zone where sulfate minerals are mainly present in the form of gypsum from the zone where sulfate minerals are mainly present in the form of anhydrite. The zone containing gypsum is usually closer to the ground surface. Water inflow into the zone containing anhydrite is critical with respect to rock swelling. Therefore, water access to the AL is considered to be an indicator for conditions leading to rock swelling in this study. Hence, the position of the AL relative to the tunnel is expected to have large influence on water access to the AL.

3. Reference model

3.1. Model domain

The model domain (Figure 3) of the reference model represents a two-dimensional vertical cross-section through the subsurface with an extent of 100 x 100 m. The reference model is set up for conditions before and after tunneling. After tunneling, there is a circular inner model boundary in the center of the model domain. This boundary marks a cylindrical tunnel cut perpendicularly to the tunnel axis (in the simulation before tunneling, this inner model boundary does not exist). The finite element mesh consists of about 5150 triangular elements and about 2700 nodes. These numbers are slightly higher in the model without tunnel because the (future) tunnel zone is part of the model domain.

[Figure 3 near here]

3.2 Geological setting and hydraulic properties

The reference model (Figure 3) represents conditions that are typically met in tunnels with swelling problems in the Triassic Gipskeuper ("Gypsum Keuper") formation [e.g., *Butscher et al.*, 2011b; *Berdugo et al.*, 2009a, 2009b]. The Gipskeuper formation is feared in tunneling, because it contains clay-sulfate rocks that are subject to heavy swelling [*Steiner*, 1993]. The geological strata associated with this formation are introduced in more detail in the case study presented in chapter 5. We assume horizontal layering of the geological units. In the middle part of the model domain, from z = 30 m to 55 m, an aquitard exists. It represents the non-weathered Gipskeuper and the underlying Lettenkeuper consisting of marlstone with interbedded clay and dolomite layers. A tunnel (center at $x = z$ = 50 m, 10 m diameter) is located in the non-weathered Gipskeuper. In the reference model, it is surrounded by a 2.5 m thick EDZ. The non-weathered Gipskeuper contains the calcium-sulfate minerals anhydrite ($CaSO_4$) below the AL, and gypsum ($CaSO_4 \cdot 2H_2O$) above the AL. The AL is located 1 m below the tunnel invert at z = 44 m.

Above the Gipskeuper aquitard, separated by the GL, an aquifer extends from z = 55 m to the ground surface at z = 100 m. This aquifer represents the weathered Gipskeuper and overlying Quaternary sediments. The weathered Gipskeuper is characterized by leaching of the sulfate minerals. A gypsum karst may have developed in the weathered Gipskeuper, providing preferential pathways for groundwater flow. Below the Gipskeuper aquitard, an aquifer follows from z = 30 m to the model bottom at z = 0 m. This aquifer represents the karstified carbonate rocks of the Upper Muschelkalk formation.

For our scenario simulations, we assume a hydraulic conductivity k = 1E-10 ms^{-1} for the aquitard, k = 1E-6 ms^{-1} for the aquifers and k = 1E-4 ms^{-1} for the EDZ. These values are based on borehole tests and modeling studies in northern Switzerland for the non-weathered Gipskeuper and Muschelkalk [*Nagra*, 2002], and increased conductivities in the weathered Gipskeuper due to karst features [*Klimchouk and Andrechuk*, 1996] and in the EDZ [*Tsang et al.*, 2005] (c.f., chapter 4.4).

3.3 Boundary conditions

The top of the model domain (ground surface) is assigned a specified head boundary condition (1st kind, Dirichlet type) with a hydraulic head h = 100 m. The bottom of the model is also a specified head boundary with a hydraulic head h = 80 m. The left and right model sides are no-flow boundaries. These boundary conditions superimpose a downward directed flow field from the land surface to depth, corresponding to the "hill position" introduced in section 2.2. The difference between the hydraulic head at the top (100 m) and bottom (80 m) of the model domain approximately matches the hydraulic gradient within the black square to the right in Figure 2, which represents this position in a simple, regional scale groundwater model.

The inner model boundary, representing the tunnel perimeter, is set as a transfer boundary condition (3rd kind, Cauchy type). Flow through this model boundary not only depends on the difference between the head assigned to the boundary and the head in the model domain, but it also depends on a transfer rate assigned to the material of the model domain at the boundary. This kind of boundary

condition was originally developed to model surface water – groundwater interaction: the exchange between a river and the groundwater depends on the river stage and the groundwater head, but is limited by a "colmation layer", leading to a certain "resistance" to flow. In our case, this transfer boundary condition is used to simulate the resistance against water outflow into the tunnel provided by the tunnel lining (Figure 4). The transfer rate r (in s^{-1}) assigned at the model boundary is the ratio of the hydraulic conductivity k_b (in ms^{-1}) of the resisting boundary layer and the thickness d (in m) of this layer:

$$r = k_b/d \tag{1}$$

Flow through this boundary is calculated according to the equation

$$Q = \int q \, dA \qquad \text{with} \tag{2}$$

$$q = r \, (h_b - h_{md}) \tag{3}$$

with Q being the flow rate (in m^3s^{-1}), q the normal flux through the area A ("Darcy velocity" in ms^{-1}), A the surface area (in m^2) through which flow Q occurs, r the transfer rate (in s^{-1}), h_b the head assigned to the boundary (representing the inner boundary of the boundary layer) and h_{md} the head in the model domain at the boundary (representing the outer boundary of the boundary layer). FEFLOW allows one to assign different transfer rates for flow into the model and flow out of the model domain (the tunnel area itself is not part of the numerical model domain, c.f. Figure 3). We set the inflow transfer rate 0 s^{-1}, i.e., there is no (negative) inflow into the model domain via this boundary because we assume that the tunnel acts as sink. In contrast, the outflow transfer rate is > 0 s^{-1}, i.e., water inflow into the tunnel is allowed. In the reference model, the outflow rate is set 2.3E-9 s^{-1}. This corresponds to a concrete lining being 1 m thick and having a hydraulic conductivity of 2.3E-9 ms^{-1}. The head we assigned to this boundary corresponds to the elevation of the boundary (hydraulic head corresponds to the elevation head; e.g., the tunnel crown at z = 55 m is assigned a head of 55 m, the invert at z = 45 m is assigned a head of 45 m, etc.). These values are based on the assumption that there is no hydrostatic pressure inside the tunnel because the tunnel is filled with air at atmospheric pressures.

[Figure 4 near here]

3.4 Visualization of simulation results

To visualize absolute values of calculated hydraulic head we plot contour lines at 2 m intervals. In addition, we show the head distribution by color fringes, where the total range of the hydraulic head in one simulation is divided into 32 equal intervals. This makes it easy to see the gradient of the hydraulic head both with respect to steepness and direction (from red - high value, to green - low value). Note that same colors indicate the same value only in one and the same simulation, but not among different simulations.

To assess water inflow into the anhydrite-bearing layers of the Gipskeuper, we track flow paths from the AL backward over a period of 10 years ("particle tracking", e.g., *Bear and Vernuijt* [1987]). The 10 year period is based on the assumption that major repairs of tunnel infrastructure are typically anticipated every 50 years. More frequent repairs are considered exceptional. The performance after a 10 year period is indicative of adequate or inadequate tunnel design. Therefore, 10 years is assumed to be the relevant order of magnitude for the time scale considered in this study. Particle tracks are calculated based on the pore velocity, given by

$$v = q/n \tag{4}$$

with v being the pore velocity (in ms^{-1}), n the effective porosity (connected porosity contributing to fluid flow), and q the Darcy velocity (in ms^{-1}; c.f. eq. 2). Particle tracking using FEFLOW is based on the same value of the effective porosity for the entire model domain. We choose a value of 0.2 for the effective porosity to represent the high conductivity units (aquifers and EDZ). The effective porosity of the aquitard (non-weathered Gipskeuper), however, is expected to be lower. Boidin et al. [2009] experimentally determined an average effective porosity of ~0.08 in samples of anhydritic marls of the Gipskeuper at a site in northeastern France. According to this value, particle tracks in the aquitard would be 2.5 times longer than calculated in this study. It is later shown, however, that the particle tracks are so short in the aquitard that they cannot be displayed in the Figures of this study. In view of this, the conclusions derived from the particle tracking are not affected by the simplifying assumption that the effective porosity is 0.2 in the entire model domain.

The AL is represented by a horizontal line that extends to the model boundaries (Figure 3: red line), and 1001 starting points of the particle tracks are distributed evenly on this line (one starting point every 0.1 m). The calculated particle tracks, later shown by blue lines (Figures 5 to 10), mark the 10-year capture zone of the AL. Water that is present in the area covered by the particle tracks flows towards the AL and reaches it within 10 years or less. The interpretation of the model results is based on the assumption that conditions for swelling are met when the capture zone of the AL (particle tracks) extends into an aquifer. In addition, we indicate the groundwater flow rates Q (in ld^{-1} per tunnel meter) at the AL under the tunnel perimeter, i.e., from x = 45 m to x = 55 m (Table 1). The flow rates are given by eq. 2 ($Q = \int q\, dA$). In this context, the area A (in m^2) is defined by the considered length of the AL (10 m from x = 45 m to x = 55 m, see Figure 3) times the depth parallel to the tunnel axis (i.e., perpendicularly to the two-dimensional model cross-section, corresponding to 1 tunnel meter). From this flow rate, we calculate the maximum volume V (in m^3) of gypsum that can be generated by the reaction $CaSO_4 + 2H_2O = CaSO_4 \bullet 2H_2O$, assuming that all water flowing through the AL is "consumed" by anhydrite to form gypsum (36 cm^3 water can react with 47 cm^3 anhydrite to form 74 cm^3 gypsum; c.f., Figure 1) and that the pore water volume does not change during the swelling process as was discussed in the introduction chapter. We give an estimate of the maximum floor heave at the tunnel invert that can result from the volume increase due to this reaction. To this end, we assume that the total rock volume increase due to the replacement of anhydrite by gypsum

(e.g., 47 cm^3 anhydrite would be replaced by 74 cm^3 gypsum if 36 cm^3 water are available, leading to an increase in rock volume of 27 cm^3; c.f., Figure 1) results only in an upward extension of the rock mass (heave) in the zone under the tunnel perimeter (we consider a 10 m wide zone perpendicular to the tunnel axis from x = 45 m to x = 55 m), i.e., an increase of 27 m^3 total rock volume leads to a floor heave of 2.7 m per unit length of the tunnel. This heave represents a theoretical, maximum heave that can be expected under available water amounts at the AL within a certain time. Nevertheless, large floor heaves exceeding 1 m are reported from several tunnels built in the Gipskeuper formation [e.g., *Steiner*, 1993].

4. Numerical simulations

4.1 Reference scenario before and after tunneling

Figure 5 shows the distribution of the hydraulic head after tunneling and the total area that is drained by the tunnel (in blue and red). Water present in the blue colored parts of this area (sub-areas 1 and 2 in Figure 5) crosses the AL when flowing towards the tunnel, whereas water present in the red colored parts (sub-areas 3 and 4) is drained by the tunnel without getting in contact with anhydrite-bearing strata. In contrast to the light-colored parts of the tunnel's drainage area (sub-areas 2 and 4), water in the dark-colored areas (sub-areas 1 and 3) reach the AL or, respectively, the tunnel within 10 years or less. In the following figures (Figures 6 to 10 and 14), only particle tracks that reach the AL within 10 years (or less) are shown to indicate the 10-year capture zone of the AL (dark blue sub-area 1 in Figure 5).

[Figure 5 near here]

Figure 6 compares the distribution of the hydraulic head and the 10-year capture zone of the AL in the reference model before (left) and after tunneling (right). Before tunneling, the gradient is downward directed (100 m at the ground surface, 80 m at the bottom of the model), perpendicular to the ground surface, and it is high in the aquitard (~0.8) and low (close to 0) in the aquifers. Because of the low hydraulic conductivity of the aquitard, the 10-year capture zone of the AL is very short (~0.1 m; it cannot be seen under the red line marking the AL in Figure 6). After tunneling, the hydraulic gradient is directed towards the tunnel. The 10-year capture zone of the AL covers the part of the EDZ that is below the AL, and extends upward along the outer boundary of the EDZ into the aquifer above the tunnel, where it forms two "wings" that reach more than 30 m into the aquifer (c.f., Figure 5). From the perspective of swelling clay-sulfate rocks, it is important to note that there is water from the aquifer above the tunnel (weathered GK) inflowing in anhydrite-containing layers at the AL within less than 10 years after tunnel excavation. The inflow is caused by the hydraulic changes induced by tunneling and can cause the transformation of anhydrite into gypsum and swelling. The calculated inflow rate at the AL under the tunnel perimeter (Table 1) is 14.1 ld^{-1} per tunnel meter (tm) after tunneling, compared to 0.1 ld^{-1} per tm before tunneling. The volume of water available at the AL under the tunnel perimeter after tunneling would be sufficient to generate 10.6 m^3 gypsum from anhydrite per year and tm, corresponding to a maximum floor heave of 38.8 cm per year. Before tunneling, only 0.05 m^3 gypsum could be created (0.2 cm heave) per year.

[Figure 6 and Table 1 near here]

4.2 Topographic position of tunnel

To see how the topographic position of a tunnel influences water inflow at the AL, we consider a "hill position" with superimposed downward directed groundwater flow, a "valley position" with superimposed upward flow, and a "slope position" with superimposed horizontal groundwater flow (c.f., Figure 2). The scenario "hill position" corresponds to the reference model. In the scenario "valley position", we rotated the superimposed flow field by 180° by setting a specified head boundary at the bottom with a head of 100 m, and another specified head boundary at the top with a head of 80 m (the boundaries at the left and right being no-flow boundaries). In the model in "slope position", we rotated the superimposed flow field by 90° by setting a specified head boundary at the right model boundary with a head of 100 m., and another specified head boundary at the left model boundary with a head of 80 m (the boundaries at the top and bottom being no-flow boundaries). Tunnel inflow can lead to drawdown of the groundwater level if groundwater recharge is less than inflow into the tunnel. The feedback of tunnel inflow on regional scale flow conditions is complex, and processes include changes in both recharge and groundwater level. By specifying a constant hydraulic head at this boundary, we make the simplifying assumption that drawdown of the groundwater level as a result of tunnel inflow is balanced by groundwater recharge in the models.

In all these scenarios the 10-year capture zone of the AL extends into the aquifer above the tunnel (Figure 7). The "wings" of the capture zone extending into the aquifer above the tunnel are slightly shorter in the scenario "valley position" compared to the reference model (corresponding to a "hill position"). In the "slope position" scenario, the capture zone forms only one "wing" extending to the right of the tunnel. In the aquifer above the tunnel, this wing is located just above the GL (i.e., it follows the base of the aquifer above the tunnel). Calculated flow rates at the AL under the tunnel perimeter (Table 1) are 17.0 ld^{-1} per tm and 9.1 ld^{-1} per tm for the "valley position" and "slope position", respectively, corresponding to the possibility to generate 12.8 m^3 and 6.8 m^3 gypsum (47.7 cm and 25.0 cm floor heave). It can be concluded, that for the assumed configuration the influence of the "superimposed" flow field on potential swelling, i.e., the influence of the position of the tunnel relative to topographic structure, is relatively low.

[Figure 7 near here]

4.3 Sealing of tunnel

It can be expected that the capability of the tunnel liner to prevent water inflow into the tunnel, i.e., its sealing capability, will strongly influence the drainage effect of the tunnel and the hydraulic conditions around the tunnel. We conducted simulations in which we reduced the transfer rate at the tunnel boundary (c.f., chapter 3.4 and equations 1 and 2) by a factor of 10 (r = 2.3E-10 s^{-1} compared to r = 2.3E-9 s^{-1} in the reference model) and by a factor of 100 (r = 2.3E-11 s^{-1}). While the 10-year capture zone of the AL extends far into the aquifer over the tunnel in the reference model, this capture

zone still reaches the aquifer in the scenario with the 10-times reduced transfer rate, but is significantly shortened (Figure 8). In the scenario with a 100-times reduced transfer rate, this capture zone remains in the EDZ surrounding the tunnel and does not extend into an aquifer. The calculated flow rates at the AL under the tunnel perimeter (Table 1) decrease from 14.1 ld^{-1} per tm (reference model) to 1.5 ld^{-1} per tm (10-times reduced transfer rate) to 0.3 ld^{-1} per tm (100-times reduced transfer rate). The estimated gypsum volumes that can be created by the water available at the AL per year are 10.6 m^3, 1.1 m^3 and 0.2 m^3, respectively, and the corresponding maximum floor heaves are 38.8 cm, 4.1 cm and 0.8 cm per year, respectively. From this it follows that the sealing of the tunnel liner strongly influences the swelling potential at the tunnel floor. In our scenarios, with the chosen configuration, swelling would almost be prevented in the scenario with 100-times reduced transfer rate (100-times increased sealing of tunnel) by strongly reducing water inflow from aquifers to anhydrite-bearing layers.

[Figure 8 near here]

4.4 Excavation damaged zone (EDZ)

It is hypothesized that an increase of rock hydraulic conductivity in the EDZ around a tunnel is an important prerequisite to provide pathways for groundwater flow. However, the hydraulic effectiveness at an actual tunnel site is usually unknown. In this study we assumed a hydraulic conductivity of c = 1E-4 ms^{-1} in the (2.5 m thick) EDZ of the reference model. This corresponds to an increase of hydraulic conductivity of 6 orders of magnitude (OM) compared to the unaltered aquitard (non-weathered Gipskeuper: k = 1E-10 ms^{-1}). An increase of 6 OM is the maximum increase estimated by *Tsang et al.* [2005] for indurated clays. We calculated a first scenario where we decreased the hydraulic conductivity in the EDZ to k = 1E-6 ms^{-1} (increase of k in the EDZ of 4 OM compared to unaltered aquitard). In this scenario, the conductivity of the EDZ corresponds to the conductivity of the aquifer above the tunnel. In a second scenario, we used a hydraulic conductivity of k = 1E-8 ms^{-1} in the part of the EDZ, which consists of non-weathered Gipskeuper rocks (increase of k in the EDZ of 2 OM compared to unaltered aquitard). The conductivity in the EDZ within the aquifer above the tunnel (c.f., Figure 3) remained at k = 1E-6 ms^{-1} in this scenario.

While the 10-year capture zone of the AL in the first scenario (k = 1E-6 ms^{-1} in EDZ) with respect to its geometry and extent does not differ much from the capture zone calculated with the reference model, the capture zone in the second scenario (k = 1E-8 ms^{-1} in the part of the EDZ consisting of non-weathered Gipskeuper) is restricted to a narrow zone in the EDZ below the AL (Figure 9). The calculated flow rates at the AL under the tunnel perimeter (Table 1) decrease from 14.1 ld^{-1} per tm (reference model) to 13.2 ld^{-1} per tm (first scenario) to 1.1 ld^{-1} per tm (second scenario) (Table 1). The corresponding gypsum volumes that can be created per year and tm at the AL are 10.6 m^3, 9.8 m^3 and 0.8 m^3, respectively, and the corresponding maximum floor heaves are 38.8 cm, 35.8 cm and 3.0 cm per year, respectively. It can be concluded that the influence of the EDZ, both on water inflow at the AL and on the swelling potential, is high. It seems that there is a "critical k" in the EDZ above which water inflow from an aquifer is possible within a certain time (here: 10 years) for the considered

configuration. For our configuration, this "critical *k*" is between 1E-6 ms^{-1} and 1E-8 ms^{-1} (i.e., between the first and second scenario), because the 10-year capture zone extends into the aquifer above the tunnel and produces high flow rates at the AL in the reference model (k = 1E-4 ms^{-1}) and the first scenario (k = 1E-6 ms^{-1}), but not in the second scenario (k = 1E-8 ms^{-1}).

[Figure 9 near here]

4.5 Geological setting

In the reference model and the scenarios so far we considered a configuration where the tunnel and its surrounding EDZ provided a "link" between the aquifer above the tunnel and the AL under the tunnel invert. In the following scenarios, we first prevent this link by considering the AL situated 4 m deeper, i.e. outside (under) the EDZ, and by considering the GL (base of the aquifer above the tunnel) situated 5 m higher, i.e., outside (above) the EDZ (Figure 10). Then we consider the GL situated 5 m higher outside the EDZ, but also a fault cutting through the tunnel area just 2.5 m right to the tunnel in contact with the EDZ. This fault provides a link between the aquifers above and under the tunnel area and the AL. We implemented the fault as a discrete linear element with additional flow parallel to this element [*Diersch*, 2009b], and assigned a hydraulic conductivity k = 1E-6 ms^{-1} and a cross sectional area of 1 m^2 to the fault. As the link between the AL and the aquifers provided by a fault would exist also before tunneling, we analyzed this configuration also without tunnel/EDZ.

[Figure 10 near here]

In both scenarios without fault, the extent of the 10-year capture zones of the AL is very short, and the capture zones do not extend into an aquifer (Figure 10 top row). In the scenario with the AL below the EDZ, the 10-year capture zone is too short to be seen in Figure 10 (top left). In the scenario with the GL above the EDZ, a short capture zone of the AL can be seen within the EDZ (Figure 10 top right). However, in the scenario with fault, the situation is different. The fault provides pathways for preferential flow and produces inflow at the AL even though the position of the GL is outside the EDZ. In this scenario, the 10-year capture zone of the AL extends into the aquifer under the tunnel in the lower model part (Figure 10 bottom left). Before tunneling, in contrast, the AL was linked via the fault to the aquifer above the tunnel in the upper model part (Figure 10 bottom right). The origin of the groundwater reaching the AL is expected to have an influence on geochemical conditions controlling anhydrite dissolution and gypsum precipitation, and thus swelling, because sulfate concentrations of groundwater in the aquifer above the tunnel (representing weathered Gipskeuper/gypsum karst) are likely to be much higher than sulfate concentrations of groundwater in the aquifer below the tunnel (representing the Upper Muschelkalk/carbonate karst).

The calculated flow rates at the AL under the tunnel perimeter (Table 1) are low for the scenarios without fault (0.1 ld^{-1} in the scenario with the deeper AL and 0.8 ld^{-1} in the scenario with the higher GL). In contrast, flow rates are very high (24.7 ld^{-1}) in the scenario after tunneling with fault. Before tunneling (but with fault), flow rates at the AL under the tunnel perimeter were low (0.1 ld^{-1}). Note

that these low flow rates are calculated for the Al under the tunnel perimeter. At the point where the fault cuts through the AL, flow rates are high also before tunneling. The corresponding volumes of gypsum that can be generated from the water inflow within one year per tm are 0.1 m^3 (scenario low AL position), 0.6 m^3 (scenario high GL position), 18.5 m^3 (scenario with fault after tunneling) and 0.04 m^3 (scenario with fault before tunneling). The corresponding maximum floor heaves per year are 0.3 cm (scenario low AL position), 2.1 cm (scenario high GL position), 67.9 cm (scenario with fault after tunneling) and 0.2 cm (scenario with fault before tunneling). These results confirm the expectation that major swelling has only to be expected if the tunnel and its surrounding EDZ "geometrically" link an aquifer with the AL, or if such a link is provided by a fault.

5. Case study

5.1 Observed swelling heaves

During construction and operation of the Chienberg tunnel in Switzerland, major problems occurred with swelling clay-sulfate rocks of the Gipskeuper. We applied the presented approach to a particular section in this tunnel (Figure 11) that crosses one of two existing swelling zones. Already during construction, a heave of the open floor of about 1.5 m was observed in this section after a three month lasting interruption of the excavation (corresponding to an average heave rate of 600 cm per year). After the installation of the lining, additional heave at the tunnel invert totaling 81 mm have been measured, before countermeasures, including an artificial deformable zone under the road surface, were successfully implemented to prevent further heave of the road surface (Kovári and Chiaverio, 2007). Yet, the swelling process in the deformable zone continues to date with heaves up to 575 mm measured within about two years (up to 25.2mm per month corresponding to an average heave rate of about 30 cm per year).

[Figure 11 near here]

5.2 Geological setting

The Chienberg tunnel crosses Triassic and Jurassic bedrock with a stratigraphic extent from the Opalinus Clay (top) to the Gipskeuper (bottom). Below these strata, the Lettenkeuper and the Muschelkalk follow (Figure 12). The strata consist of alternating shale and carbonate rock with various hydraulic permeabilities. In the cross-section under consideration (Figure 13), the tunnel is situated in the Gipskeuper, consisting of a dark grey marlstone and interbedded layers of clay and dolomite. The Gipskeuper contains anhydrite and gypsum as veins (gypsum only), lenses and nodules, as well as dispersed in the rock matrix and as massive beds. The anhydrite level (AL) was determined to be ~5.5 m above the tunnel invert on the basis of mineralogical analyses of core samples taken from exploration boreholes. The gypsum level (GL), marking the boundary weathered/non-weathered Gipskeuper, was found to be located at the level of the tunnel crown during excavation in this section. The weathered Gipskeuper is characterized by a leaching of the sulfate minerals accompanied by rock softening, resulting in soil-like geotechnical properties with low rock stability and a "crumbly" appearance. A gypsum karst may have developed in the weathered Gipskeuper, providing preferential pathways for groundwater flow. During tunnel excavation, water

inflow from the weathered Gipskeuper into the tunnel has often been observed, with flow rates up to 60 $lmin^{-1}$ at some places. The water present in the weathered Gipskeuper is impounded by the underlying non-weathered Gipskeuper, which acts as an aquitard. The rocks of the Bunte Mergel above the Gipskeuper are very similar to those of the Gipskeuper when weathered, and both units are hardly distinguishable from each other in drill cuttings.

[Figures 12 and 13 near here]

During tunnel construction, a cave-in occurred. The cave-in area above the tunnel is filled with loose material consisting of weathered Gipskeuper, Bunte Mergel and Quaternary rocks. A gallery left of the tunnel (c.f., Figure 13) was excavated after the cave-in to explore and secure the caved-in area. It was then re-filled with material from the tunnel excavation.

5.3 Groundwater modeling

Model setup

The model domain of the case study corresponds to the geological cross-section shown in Figure 13. *Butscher et al.* [2011b] presented a groundwater model of this cross-section. In the present study, model properties and boundary conditions have been chosen differently, namely along the lines of the synthetic scenario simulations presented in chapter 4. Aquifers (i.e., all weathered strata, Quaternary, Muschelkalk aquifer) have a hydraulic conductivity k = 1E-6 ms^{-1}; other strata (aquitards) have a hydraulic conductivity k = 1E-10 ms^{-1}. The cave-in area and the filled-in exploration gallery next to the tunnel are assigned a hydraulic conductivity k = 1E-3 ms^{-1}. Faults were implemented as linear elements having a hydraulic conductivity k = 1E-6 ms^{-1} parallel to the fault and a cross-sectional area of 1 m^2. The hydraulic conductivity of the EDZ was set either at k = 1E-4 ms^{-1} (corresponding to the reference model) or k = 1E-8 ms^{-1} (corresponding to the second scenario in chapter 4.4), depending on the scenario.

The upper model boundary (ground surface) is a specified head boundary (1st kind, Dirichlet type) with the hydraulic head corresponding to the elevation. The lower model boundary was assigned a specified head having a constant value of 465 m. This value was taken from a regional scale model of the area [*Butscher et al.*, 2011a]. The regional scale model crosses the Chienberg tunnel in a similar direction at a position near the here considered cross-section. The model boundaries at the sides are no-flow boundaries. The tunnel was implemented as a transfer boundary (3rd kind, Cauchy type) with the hydraulic head corresponding to the elevation of the tunnel perimeter. Outflow transfer rates were chosen to be r = 2.3E-9 s^{-1} (corresponding to the reference model) and r = 2.3E-11 s^{-1} (sealing effect of the tunnel liner) depending on the scenario (inflow transfer rate = 0).

Just as in the synthetic scenario simulations in chapter 4, we show the 10-year capture zone of the AL by tracking back particles. We use 201 evenly distributed starting points on the AL extending from 10 m to the left of the tunnel axis to 10 m right of the tunnel axis (i.e., one starting point every 0.1 m). In addition, we show contour lines of the hydraulic head in 2 m intervals.

Results

Before tunneling (Figure 14 top left), the hydraulic gradient at the AL is generally upward directed in the (future) tunnel zone with a horizontal component from S to N. The 10-year capture zone extends only a few cm (too short to be displayed in the Figure). The calculated flow rate at the AL (Table 2) is very low (0.02 ld^{-1} per tm). The available water inflow at the AL potentially produces 0.01 m^3 gypsum from anhydrite per year and tm, corresponding to a maximum floor heave of 0.03 cm per year. After tunneling (Figure 14 top right), considering a hydraulic conductivity k = 1E-4 ms^{-1} in the EDZ (increase of 6 OM compared to unaltered Gipskeuper) and a transfer rate of r = 2.3E-9 s^{-1} at the tunnel boundary, we can observe a 10-year capture zone of the AL extending into the aquifer (weathered Keuper strata and Quaternary) above the tunnel to the ground surface. This capture zone is divided by the tunnel into two "wings", similar to the simulations with the synthetic models (chapter 4). Water inflow at the AL (Table 2) is as high as 170.0 ld^{-1} per tm, allowing the generation of 127.6 m^3 gypsum from anhydrite per year and tm, and a maximum floor heave of 233.6 cm per year. If we reduce the hydraulic conductivity of the EDZ by a factor of 10,000 (hydraulic conductivity of 1E-8 ms^{-1}, corresponding to an increase of 2 OM compared to unaltered Gipskeuper), the geometry and extent of the 10-year capture zone are very similar to the scenario with a hydraulic conductivity k = 1E-4 ms^{-1} in the EDZ (Figure 14 bottom left), only that the two "wings" originating left and right of the tunnel are wider in the scenario with higher conductivities in the EDZ (Figure 14 top right) than in the scenario with lower conductivities in the EDZ (Figure 14 bottom left). The flow rate at the AL (Table 2), however, is reduced to 33.2 ld^{-1} per tm, allowing the generation of 24.9 m^3 gypsum from anhydrite per year and tm, and a maximum floor heave of 45.5 cm per year. If we keep the hydraulic conductivity of the EDZ at k = 1E-4 ms^{-1} but decrease the outflow transfer rate at the tunnel boundary by a factor of 100 (r = 2.3E-11 s^{-1}), the observed 10-year capture zone of the AL forms only one "wing" that is limited to a narrow area to the right of the tunnel, but the capture zone is still extending into the aquifer above the tunnel until the ground surface (Figure 14 bottom right). The flow rate at the AL (Table 2) is greatly reduced to 1.8 ld^{-1} per tm, allowing the generation of only 1.4 m^3 gypsum from anhydrite per year and tm, and a maximum floor heave of 2.5 cm per year.

[Figure 14 near here]

Interpretation

The simulations suggest that both the hydraulic conductivity of the EDZ and the outflow transfer rate ("sealing of tunnel") have strong influence on water inflow at the AL and swelling of the tunnel floor. Estimated flow rates and heaves are particularly sensitive to the assumed outflow transfer rate at the tunnel boundary. The estimated maximum floor heaves of the simulations match with the order of magnitude of field data. After excavation, but before the open space was lined, a heave corresponding to 600 cm per year was observed in the investigated tunnel section. The "open tunnel" corresponds to a situation with an outflow rate much higher than we assumed. After completion of the tunnel, floor heave corresponding to an average of 30 cm per year has been measured. This heave rate is very similar to our scenario with a hydraulic conductivity of the EDZ of k = 1E-8 ms^{-1} and an outflow

transfer rate of r = 2.3E-9 s^{-1} at the tunnel boundary. Of course, other combinations of hydraulic properties of the EDZ, the geological units and the tunnel boundary possibly result in similar heaves. However, the simulations show two important points: (1) The hydraulic properties of the EDZ have strong influence on swelling but are hardly known in practice; and (2) the lining of the tunnel, which was the most influencing factor affecting swelling in our study, should be installed as soon as possible after excavation, and the sealing of the tunnel should be improved by placement of membranes or by injection of grout behind the tunnel lining in order to minimize swelling.

6. Concluding remarks

In this study the impact of different hydrogeological factors on the swelling potential of clay-sulfate rocks was systematically investigated. The factors included the topographic setting, the EDZ around the tunnel, the sealing properties of the tunnel liner and the geological setting. Scenario simulations of synthetic situations were complemented by a case study. The results suggest that all of the investigated factors influence water inflow to anhydrite-bearing layers in the tunnel zone and, thus, rock swelling. The influence of the different factors varies depending on overall conditions. In general, the sealing ability of the tunnel liner was found to be a major factor influencing water inflow into the tunnel zone. The study underlines the importance of adequate geological and hydraulic information on the site, including the hydraulic properties of the EDZ and the tunnel liner, which are needed to assess the risk of swelling.

Swelling deformation (heave) can be reduced by a mechanical resistance (rock anchors, reinforced lining, etc.). This process is not included in the present study, and calculated heaves in this study are rather a measure of the swelling potential than an actual calculation of expected deformation. Heave-pressure-time relations are needed when the mechanical interaction between the swelling rock and the tunnel are to be evaluated. For clay-sulfate rocks, however, such relations are only known to a limited extent [e.g. *Pimentel*, 2007b]. In addition to opposing swelling deformation by mechanical resistance, engineering strategies to counter the swelling problem include the reduction of swelling pressure by allowing deformation in designated areas [*Pierau and Kiehl*, 1996]. *Kovári and Chiaverio* [2007] combined both strategies and showed how swelling pressures can be controlled by allowing limited deformation in a deformable zone under the tunnel. *Anagnostou et al.* [2010] suggested the use of hydraulic-mechanical-chemical coupled models to assess the interaction of rock swelling with the tunnel. The coupling of hydraulic, mechanical and chemical processes involved in the swelling of clay-sulfate rocks is still not sufficiently understood and requires more attention in future work.

Groundwater flow is a three-dimensional problem. Therefore, future research is needed that will investigate the influence of tunneling on groundwater flow not only in a direction perpendicularly to the tunnel axis. Particularly, flow parallel to the tunnel axis is suggested to be an important subject of future studies. In the case of a vertical arrangement of aquifers and aquitards, tunnel parallel flow is likely to connect aquifers that have been separated before tunneling. Such hydraulic changes can lead to water inflow into anhydrite-bearing layers and swelling in the vicinity of the tunnel and, in certain circumstances, even in distant strata with long-term consequences that are difficult to foresee.

Another aspect that is only considered to a minor degree so far is the time-scale at which the simulated hydraulic processes are active. For example, one wants to know if major water inflow into the AL can be prevented by installing the liner immediately after excavation (e.g., within one day), or if water inflow into the AL is about the same if, at first, a few hundred tunnel meters are excavated, before the liner is installed after some weeks. Future research involving transient models could address this issue more comprehensively.

The application of the presented approach to actual engineering projects will require a sound hydrogeological data basis. This includes knowledge of the geological configuration (including the area under the tunnel invert), hydraulic properties of geological units and engineering structure, and hydraulic boundary conditions from head measurements at different levels. If this information is provided, the effect of tunneling on hydraulic conditions in the subsurface can be well described using numerical groundwater models. With such models, one can analyze situations that are critical with respect to the swelling of clay-sulfate rocks by calculating changes in hydraulic conditions induced by tunneling that lead to water inflow into anhydrite-containing layers.

Acknowledgements

The authors thank the Tiefbauamt Basel-Landschaft (Cantonal Civil Engineering Office) for the provision of geological, hydrological and geotechnical data from the test site. This research was funded by a grant to C. Butscher from the Swiss National Science Foundation (SNF grant no. PBBSP2-130955).

References

Alonso, E.E., and S. Olivella (2008), Modelling Tunnel Performance in Expansive Gypsum Claystone, *The 12th International Conference of International Association for Computer Methods and Advances in Geomechanics (IACMAG)*, 1–6 October, 2008, Goa, India, pp. 891–910.

Anagnostou, G. (1992), Untersuchungen zur Statik des Tunnelbaus in quellfähigem Gebirge, PhD thesis, Institute for Geotechnical Engineering, ETH Zurich, Zurich Switzerland.

Anagnostou, G., E. Pimentel, and K. Serafeimidis (2010), Swelling of sulphatic claystones – some fundamental questions and their practical relevance, *Geomechanics and Tunnelling*, *3*(5), 567–572.

Azam, S. (2007), Study on the geological and engineering aspects of anhydrite/gypsum transition in the Arabian Gulf coastal deposits, *Bulletin of Engineering Geology and the Environment*, *66*, 177–185.

Bear, J., and A. Vernuijt, 1987, *Modeling groundwater flow and pollution*, Reidel Publishing Company, Dordrecht, Netherlands.

Berdugo, I.R., E.E. Alonso, E. Romero, and A. Gens (2009a), Tunnelling and swelling in Triassic sulphate-bearing rocks. Part I – Case studies from Baden-Württemberg, *Revista Epsilon*, *12*, 1–17.

Berdugo, I.R., E.E. Alonso, E. Romero, and A. Gens (2009a), Tunnelling and swelling in Triassic sulphate-bearing rocks. Part II – Case studies from Jura Mountains. *Revista Epsilon*, *12*, 18–30.

Bitterli-Brunner, P., and H. Fischer (1988), Explanations to geological map Blatt Arlesheim 1067 (in German), *Geological Atlas of Switzerland*, Bern, Switzerland.

Blount, C. W., and F. W. Dickson (1973), Gypsum-anhydrite equilibria in the system $CaSO_4$–H_2O and $CaSO_4$–NaCI–H_2O, *American Mineralogist*, *58*, 323–331.

Blümling, P., F. Bernier, P. Lebon, and C. D. Martin (2007), The excavation damaged zone in clay formations – time-dependent behaviour and influence on performance assessment, *Physics and Chemistry of the Earth*, *32*, 588–

599.

Boidin, E., F. Homand, F. Thomas, and J. Yvon (2009), Anhydrite–gypsum transition in the argillites of flooded salt workings in eastern France, *Environmental Geology*, *58*, 531–542.

Butrón, C., G. Gustafson, Å. Fransson, and J. Funehag (2010), Drip sealing of tunnels in hard rock: A new concept for the design and evaluation of permeation grouting, *Tunnelling and Underground Space Technology*, *25*, 114–121.

Butscher, C., P. Huggenberger, and E. Zechner (2011a), Impact of tunneling on regional groundwater flow and implications for swelling of clay-sulfate rocks, *Engineering Geology*, *117*, 198–206.

Butscher, C., P. Huggenberger, E. Zechner, and H. H. Einstein (2011b), Relation between hydrogeological setting and swelling potential of clay-sulfate rocks in tunneling, *Engineering Geology*, manuscript accepted pending minor revisions.

Caine, J. S., J. P. Evans, and C. B. Forster (1996), Fault zone architecture and permeability structure, *Geology*, *24*(11), 1025–1028.

Caputo, M., and H.-P. Huez (1987), Tunnel Waterproofing Using Polymeric Membranes, *Tunnelling and Underground Space Technology*, *2*(1), 83–88.

Diersch, H.-J. G. (2009a), *FEFLOW - Finite Element Subsurface Flow & Transport Simulation System, Reference Manual*, DHI-WASY GmbH, Berlin, Germany.

Diersch, H.-J. G. (2009b), Discrete feature modeling of flow, mass and heat transport processes by using FEFLOW, in *FEFLOW - Finite Element Subsurface Flow & Transport Simulation System, White Papers*, vol. 1, pp. 151–198, DHI-WASY GmbH, Berlin, Germany.

Einstein, H. H. (1996), Tunnelling in difficult ground – Swelling behaviour and identification of swelling rocks, *Rock mechanics and rock engineering*, *29*(3), 113–124.

Flückiger, A., R. Nüesch, and F. Madsen (1994), Anhydritquellung, in *Berichte der Deutschen Ton- und Tonmineralgruppe DTTG*, Band 3, edited by E. E. Kohler, pp. 146–153, J. F. Wagner, Trier, Germany.

Freeze, R. A., and P. A. Witherspoon (1967), Theoretical analysis of regional groundwater flow, 2. Effect of water-table configuration and subsurface permeability variation, *Water Resources Research*, *3*(2), 623–634.

Hauber, L., P. Jordan, F. Madsen, R. Nüesch, and B. Vögtli (2005), Clay minerals and sulfates as source of swelling of sediments, Reasons and effects of swelling, *Final report of research projects 55/92 and 52/96*, Swiss Federal Roads Office (ASTRA), Bern, Switzerland.

Hubbert, M. K. (1940), The theory of ground-water motion, *Journal of Geology*, *48*(8), 785–944.

Klimchouk, A., and V. Andrechuk (1996), Environmental problems in gypsum karst terrains, *International Journal of Speleology, 25*(3–4), 145–156.

Kovári, K., and F. Chiaverio (2007), Modular yielding support for tunnels in heavily swelling rock. *Proceedings STUVA Conference 07*, 26–29 November 2007, Cologne, Germany.

Madsen, F.T., and M. Vonmoos (1989), The swelling behaviour of clays. *Applied Clay Science*, *4*, 143–156.

Murray, R.C. (1964), Origin and diagenesis of gypsum and anhydrite, *Journal of Sedimentary Petrology*, *34*(3), 512–523.

Nagra (2002), Project Opalinuston: Synthesis of geoscientific investigation results (in German), *Nagra Technical Reprot (NTB)* 02-03, Nagra, Baden, Switzerland.

Noher, H.P., M. Meyer, and R.M. Zeh (2010), The anhydrite surface – cause of problems in tunnel constructions (new results based on measurements and observations), in *Rock Mechanics in Civil and Environmental Engineering*, edited by J. Zhao, V. Labiouse, J.-P. Dudt, and J.-F. Mathier, Taylor & Francis Group, London, UK.

Nüesch, R., W. Steiner, and F. T. Madsen (1995), Long time swelling of anhydritic rocks: mineralogical and microstructural evaluation, in *International Congress on Rock Mechanics – Proceedings*, vols. 1 and 2, edited by T. Fujii, pp. 133–138, A. A. Balkema, Rotterdam, Netherlands.

Pearson, F.J., W. Balderer, H. H. Loosli, B. E. Lehmann, A. Matter, T. Peters, H. Schmassmann, and A. Gautschi (1991), *Applied Isotope Hydrogeology – a case study in northern Switzerland*, Elsevier, Amsterdam, Netherlands.

Piereau, B., and J.R. Kiehl (1996), Widerstands- und Ausweichprinzip: Vergleich zweier Entwurfsmethoden für Tunnelbauten in quellfähigem Gebirge, *Taschenbuch für den Tunnelbau*, Verlag Glückauf GmbH, Essen, Germany.

Pimentel, E. (2007a), Quellverhalten von Gesteinen – Erkenntnisse aus Laboruntersuchungen, Quellprobleme in der

Geotechnik, *Mittelungen der Schweizerischen Gesellschaft für Boden- und Felsmechanik*, *154*, 13–20.

Pimentel, E. (2007b), A laboratory testing technique and a model for the swelling behavior of anhydritic rock, in *The second half century of rock mechanics*, vol. 1, edited by C. Olalla , N. Grossmann , and L. Ribeiro e Sousa, pp. 143–146, Taylor & Francis Group, London, UK.

Ping, X., and J. Beaudoin (1992), Mechanism of sulphate expansion, *Cement and Concrete Research*, *22*, 631–640.

Sato, T., T. Kikuchi, and K. Sugihara (2000), In-situ experiments on an excavation disturbed zone induced by mechanical excavation in Neogene sedimentary rock at Tono mine, central Japan, *Engineering Geology*, *56*, 97–108.

Steiner, W. (1993), Swelling rock in tunnels: Characterization, effect of horizontal stresses and Construction Procedures, *International Journal of Rock Mechanics & Mining Sciences & Geomechanical Abstracts*, *30*(4), 361–380.

Tóth, J. (1962), A theory of groundwater motion in small drainage basins in Central Alberta, Canada, *Journal of Geophysical Research*, *67*, 4375–4387.

Tóth, J. (1963), A theoretical analysis of groundwater flow in small drainage basins, *Journal of Geophysical Research*, *68*, 4795–4812.

Tsang, C.F., F. Bernier, and C. Davies (2005), Geohydromechanical processes in the Excavation Damaged Zone in crystalline rock, rock salt, and indurated and plastic clays – in the context of radioactive waste disposal, *International Journal of Rock Mechanics & Mining Sciences*, *42*(1), 109–125.

Wittke, W. (2007), New high-speed railway lines Stuttgart 21 and Wendlingen-Ulm - Approximately 100 km of tunnels, in *Underground Space – The 4th Dimension of Metropolises*, Proceedings of the World Tunnel Congress 2007 and 33rd ITA/AITES Annual General Assembly, Prague, May 2007, edited by J. Bartak, I. Hrdina, G. Romancov, and J. Zlamal, pp. 771–778, Taylor & Francis, London, UK.

Yilmaz, I. (2001), Gypsum/anhydrite: some engineering problems, *Bulletin of Engineering Geology and the Environment*, *59*, 227–230.

Zijl, W. (1999), Scale aspects of groundwater flow and transport systems, *Hydrogeology Journal*, *7*, 139–150.

Figure Captions

Figure 1: Mass and volume balance of the transformation of anhydrite into gypsum caused by water inflow in an open system. In clay-sulfate rocks, an inflow of 36 cm^3 water can lead to a maximum increase of total rock volume of 27 cm^3, provided that the pore water volume is constant and sufficient (47 cm^3) anhydrite is present and transformed into (74 cm^3) gypsum.

Figure 2: Influence of topography on flow pattern in homogeneous, isotropic ground (contour lines of hydraulic head in black, flow lines in blue). Groundwater flow is downward directed under hills ("hill position"), upward directed under valleys (valley position") and horizontal in between ("slope position").

Figure 3: Illustration of model setup of reference model (left) and corresponding geological setting and hydro-stratigraphy (right).

Figure 4: Calculation of tunnel inflow Q based on normal flux q ("Darcy velocity") at the tunnel perimeter, represented by a transfer boundary condition (3rd kind, Cauchy type). A: area through which flow occurs; r: transfer rate, d: thickness of resisting boundary layer (tunnel liner), h_{md}: hydraulic head in model domain at boundary layer, h_b: hydraulic head assigned to transfer boundary (correspond to elevation head), k_{md}: hydraulic conductivity of model domain (rock), k_b: hydraulic conductivity of resisting boundary layer (tunnel liner).

Figure 5: Hydraulic head field (black lines) and area drained by the tunnel (blue and red lines). Water in sub-areas 1 and 2 (blue) crosses the AL when flowing towards the tunnel, water in sub-areas 3 and 4 (red) is drained by the tunnel without crossing the AL. Water in sub-areas 1 and 3 (dark-colored) reach the AL or the tunnel within 10 years or less, water in sub-areas 2 and 4 (light-colored) needs more than 10 years to reach the AL or the tunnel.

Figure 6: Hydraulic head field (black lines and color scale) and 10-year capture of the anhydrite level (blue lines) calculated with the reference model before (left) and after tunneling (right). Before tunneling, the 10-year capture zone is so short that it cannot be seen under the red line marking the AL. After tunneling, the 10-year capture zone of the AL covers the part of the EDZ that is below the AL, and extends upward along the outer boundary of the EDZ into the aquifer above the tunnel, where it forms two "wings" that reach more than 30 m into the aquifer. Anhydrite in getting in contact with this water can transform into gypsum, triggering rock swelling.

Figure 7: Influence of topographic position on hydraulic conditions after tunneling (contour lines of hydraulic head in black, 10-year capture zone in blue). The left figure corresponds to a "valley position" (c.f., Figure 2), the right figure corresponds to a "slope position". The reference model (Figure 6 right) corresponds to a "hill position". In all positions, water from the aquifer above the tunnel reaches the AL within (less than) 10 years, which can result in the transformation of anhydrite into gypsum and rock swelling.

Figure 8: Influence of tunnel sealing on hydraulic conditions after tunneling (contour lines of hydraulic head in black, 10-year capture zone in blue). The left figure corresponds to an outflow transfer rate of 2.3E-10 s^{-1} at the tunnel boundary, the right figure corresponds to an outflow transfer rate of 2.3E-11 s^{-1}. The reference model (Figure 6 right) corresponds to an outflow transfer rate of 2.3E-9 s^{-1}. In the scenario with an outflow transfer rate of 2.3E-11 s^{-1} (right figure), water from the aquifer above the tunnel does not reach the AL within (less than) 10 years, preventing the transformation of anhydrite into gypsum and rock swelling.

Figure 9: Influence of EDZ on hydraulic conditions after tunneling (contour lines of hydraulic head in black, 10-year capture zone in blue). The left figure corresponds to a hydraulic conductivity of 1.0E-6 ms^{-1} within the EDZ, the right figure corresponds to a hydraulic conductivity of 1.0E-8 ms^{-1}. The reference model (Figure 6 right) corresponds to a hydraulic conductivity of 1.0E-4 ms^{-1}. In the scenario with a hydraulic conductivity of 1.0E-8 ms^{-1} within the EDZ (right figure), water from the aquifer above the tunnel does not reach the AL within (less than) 10 years, preventing the transformation of anhydrite into gypsum and rock swelling.

Figure 10: Influence of geological configuration on hydraulic conditions after tunneling (contour lines of hydraulic head in black, 10-year capture zone in blue). The top two figures correspond to a configuration where the anhydrite level (AL) is not linked to the aquifer above the tunnel by the EDZ (i.e., in the left figure, the AL is situated below (outside) the EDZ, in the right figure, the base of the aquifer above the tunnel is situated above (outside) the EDZ). In both cases, water from the aquifer above the tunnel does not reach the AL within (less than) 10 years, preventing the transformation of anhydrite into gypsum and rock swelling. The bottom two figures correspond to a situation, where a fault provides a link between an aquifer and the AL (left after tunneling, right before tunneling). The fault allows water access to the AL both before and after tunneling, which can result in the transformation of anhydrite into gypsum and rock swelling.

Figure 11: Location of study site.

Figure 12: Schematic, stratigraphic section also showing hydrogeological characteristics of the study area (modified from Bitterli-Brunner and Fischer, 1988; Pearson et al., 1991). Grey arrow indicates stratigraphic extent of synthetic situations, black arrow of case study. Abbreviations of geological units: Q: Quaternary, Opa: Opalinus Clay, UL: Upper Lias, Obt: Obtusus Clay, AK: Arietenkalk, UpBM: Upper Bunte Mergel, GD: Gansinger Dolomite, BM: Bunte Mergel, GK: Gipskeuper, LK: Lettenkeuper, MKaqf: Muschelkalk aquifer, MKaqt: Muschelkalk aquitard.

Figure 13: Cross-section of case study (abbreviations of geological units see Figure 12, "w" after geological unit indicates that this unit is weathered) [after *Butscher et al.*, 2011b]. Black lines indicate exploration drill holes. Dots indicate sulfate analysis samples (green: sulfate present as gypsum, red: sulfate present as anhydrite, orange: sulfate present as gypsum and anhydrite). Red line indicates anhydrite level. Dotted areas represent a cave-in area and a exploration gallery.

Figure 14: Hydraulic head field (black lines) and 10-year capture zone (blue lines) of the anhydrite level (red bar) calculated with the groundwater model of the case study. Top left: conditions before tunneling (the 10-year capture zone is too short to be displayed). Top right: Conditions after tunneling assuming a hydraulic conductivity of 1.0E-4 ms^{-1} in the EDZ and an outflow transfer rate of 2.3E-9 s^{-1} at the tunnel boundary (the values correspond to the reference model of chapter 4). Bottom left: Corresponds to figure top right, but hydraulic conductivity in EDZ is decreased by a factor of 10,000 to 1.0E-8 ms^{-1}. Bottom right: Corresponds to figure top right, but outflow transfer rate at tunnel boundary is decreased by a factor of 100 to 2.3E-11 s^{-1}, representing the sealing effect of the tunnel liner. In all scenarios, water from the aquifer above the tunnel reaches the AL within (less than) 10 years after tunneling, which can result in the transformation of anhydrite into gypsum and rock swelling. In the sceanrios with a decreased hydraulic conductivity of the EDZ and decrease outflow transfer rate at the tunnel boundary (bottom row), the 10-year capture zone is narrower than in the reference situation (top right), indicating reduced water access to the AL which can result in reduced transformation of anhydrite into gypsum and reduced rock swelling.

Tables

Table 1: Flow rates at anhydrite level (AL), maximum volume of gypsum created per year due to the transformation of anhydrite into gypsum and corresponding maximum floor heave per year calculated for different scenarios of synthetic situations.

Scenario	Flow rate at AL under tunnel perimeter (ld^{-1}) per tm	Max. Volume of gypsum created under tunnel perimeter per year and tm (m^3)	Max. floor heave per year (cm)
Reference model			
before tunneling	0.07	0.05	0.19
after tunneling (k_{EDZ}:1E-4ms^{-1}, r:2.3E-9s^{-1})	14.11	10.59	38.77
Topography			
Valley position	17.00	12.75	46.71
Slope position	9.10	6.83	25.01
Sealing			
Increase factor 10 (r:2.3E-10s^{-1})	1.51	1.13	4.14
Increase factor 100 (r:2.3E-11s^{-1})	0.27	0.20	0.75
EDZ			
Decrease factor 100 (k_{EDZ}:1E-6ms^{-1})	13.02	9.77	35.77
Decrease factor 10,000 (k_{EDZ}:1E-8ms^{-1})	1.10	0.83	3.03
Geology			
AL below EDZ	0.12	0.09	0.33
GL above EDZ	0.79	0.59	2.16
GL above EDZ + fault	24.71	18.54	67.89
GL above EDZ + fault before tunneling	0.05	0.04	0.15

Table 2: Flow rates at anhydrite level (AL), maximum volume of gypsum created per year due to the transformation of anhydrite into gypsum and corresponding maximum floor heave per year calculated for different scenarios of the case study.

Scenario	Flow rate at AL under tunnel perimeter (ld^{-1}) per tm	Max. Volume of gypsum created under tunnel perimeter per year and tm (m^3)	Max. floor heave per year (cm)
Reference model			
before tunneling	0.02	0.01	0.03
after tunneling (k_{EDZ}:1E-4ms^{-1}, r:2.3E-9s^{-1})	170.00	127.55	233.55
EDZ			
Decrease factor 10000 (k_{EDZ}:1E-8ms^{-1})	33.15	24.87	45.54
Sealing			
Increase factor 100 (r:2.3E-11s^{-1})	1.83	1.38	2.52

Figures

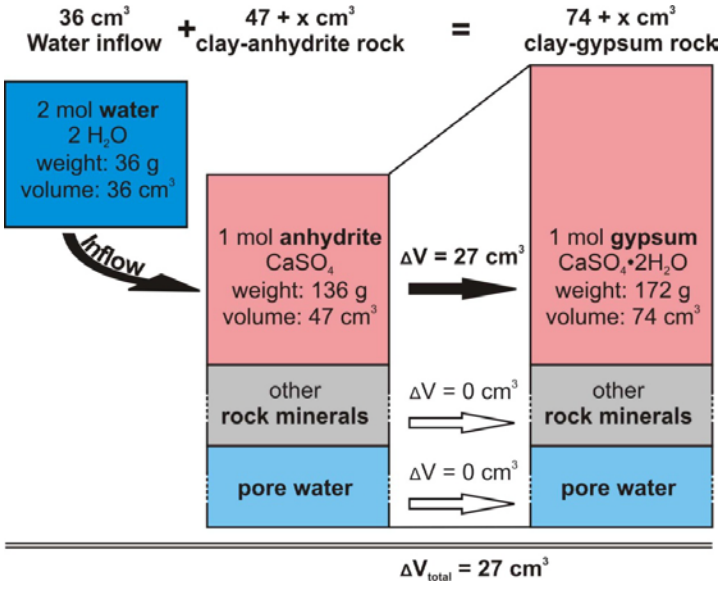

Figure 1: Mass and volume balance of the transformation of anhydrite into gypsum caused by water inflow in an open system. In clay-sulfate rocks, an inflow of 36 cm^3 water can lead to a maximum increase of total rock volume of 27 cm^3, provided that the pore water volume is constant and sufficient (47 cm^3) anhydrite is present and transformed into (74 cm^3) gypsum.

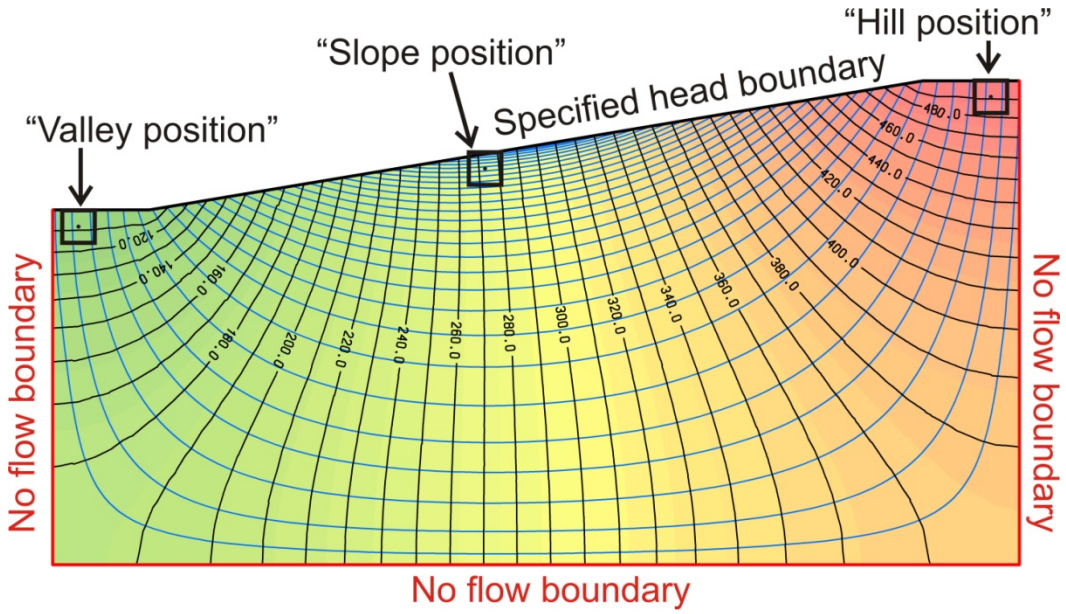

Figure 2: Influence of topography on flow pattern in homogeneous, isotropic ground (contour lines of hydraulic head in black, flow lines in blue). Groundwater flow is downward directed under hills ("hill position"), upward directed under valleys (valley position") and horizontal in between ("slope position").

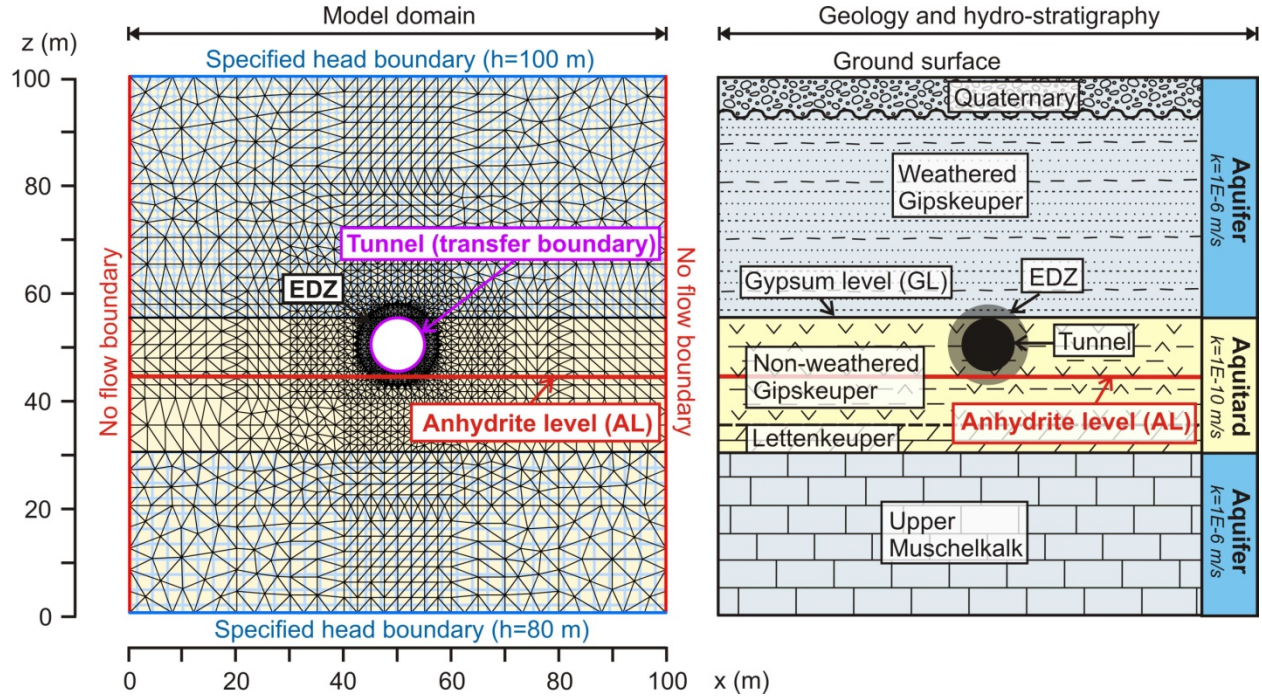

Figure 3: Illustration of model setup of reference model (left) and corresponding geological setting and hydro-stratigraphy (right).

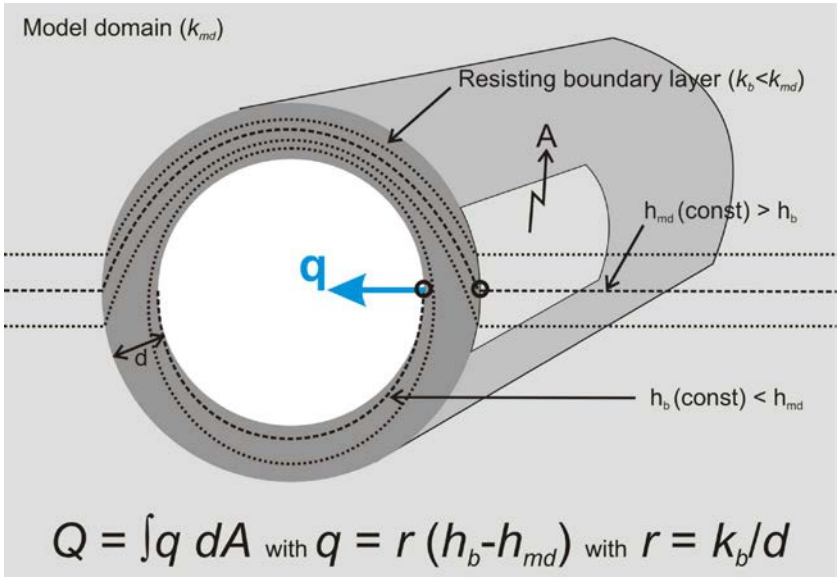

Figure 4: Calculation of tunnel inflow Q based on normal flux q ("Darcy velocity") at the tunnel perimeter, represented by a transfer boundary condition (3rd kind, Cauchy type). A: area through which flow occurs; r: transfer rate, d: thickness of resisting boundary layer (tunnel liner), h_{md}: hydraulic head in model domain at boundary layer, h_b: hydraulic head assigned to transfer boundary (correspond to elevation head), k_{md}: hydraulic conductivity of model domain (rock), k_b: hydraulic conductivity of resisting boundary layer (tunnel liner).

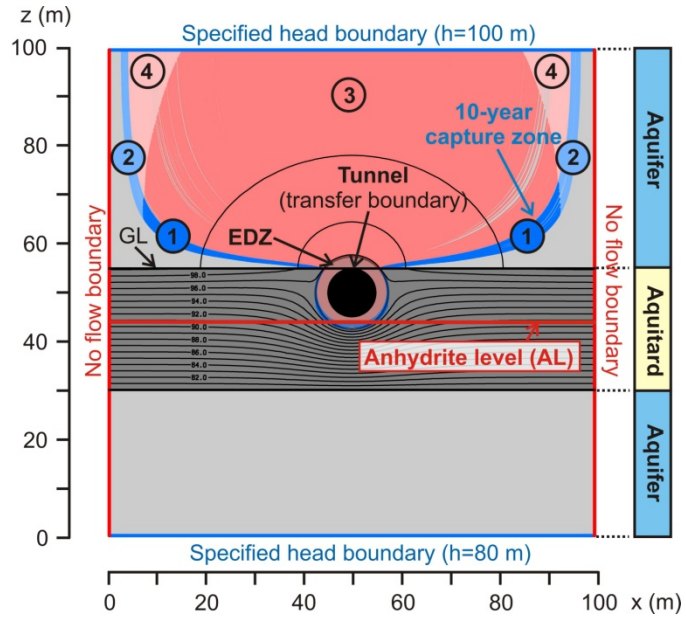

Figure 5: Hydraulic head field (black lines) and area drained by the tunnel (blue and red lines). Water in sub-areas 1 and 2 (blue) crosses the AL when flowing towards the tunnel, water in sub-areas 3 and 4 (red) is drained by the tunnel without crossing the AL. Water in sub-areas 1 and 3 (dark-colored) reach the AL or the tunnel within 10 years or less, water in sub-areas 2 and 4 (light-colored) needs more than 10 years to reach the AL or the tunnel.

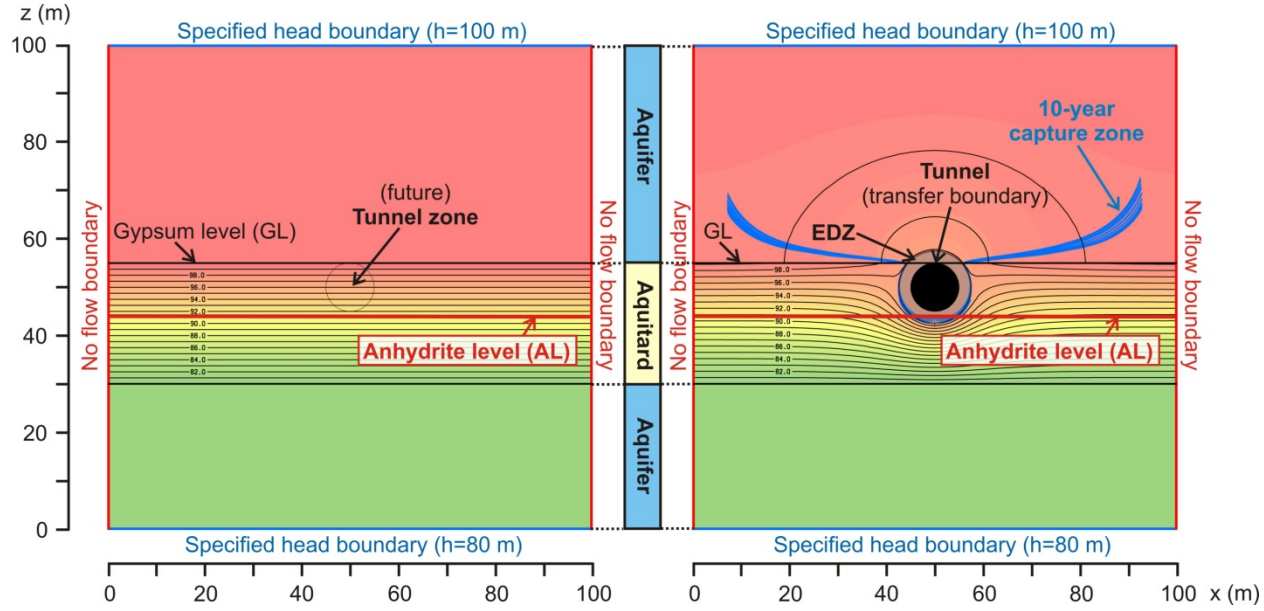

Figure 6: Hydraulic head field (black lines and color scale) and 10-year capture of the anhydrite level (blue lines) calculated with the reference model before (left) and after tunneling (right). Before tunneling, the 10-year capture zone is so short that it cannot be seen under the red line marking the AL. After tunneling, the 10-year capture zone of the AL covers the part of the EDZ that is below the AL, and extends upward along the outer boundary of the EDZ into the aquifer above the tunnel, where it forms two "wings" that reach more than 30 m into the aquifer. Anhydrite in getting in contact with this water can transform into gypsum, triggering rock swelling.

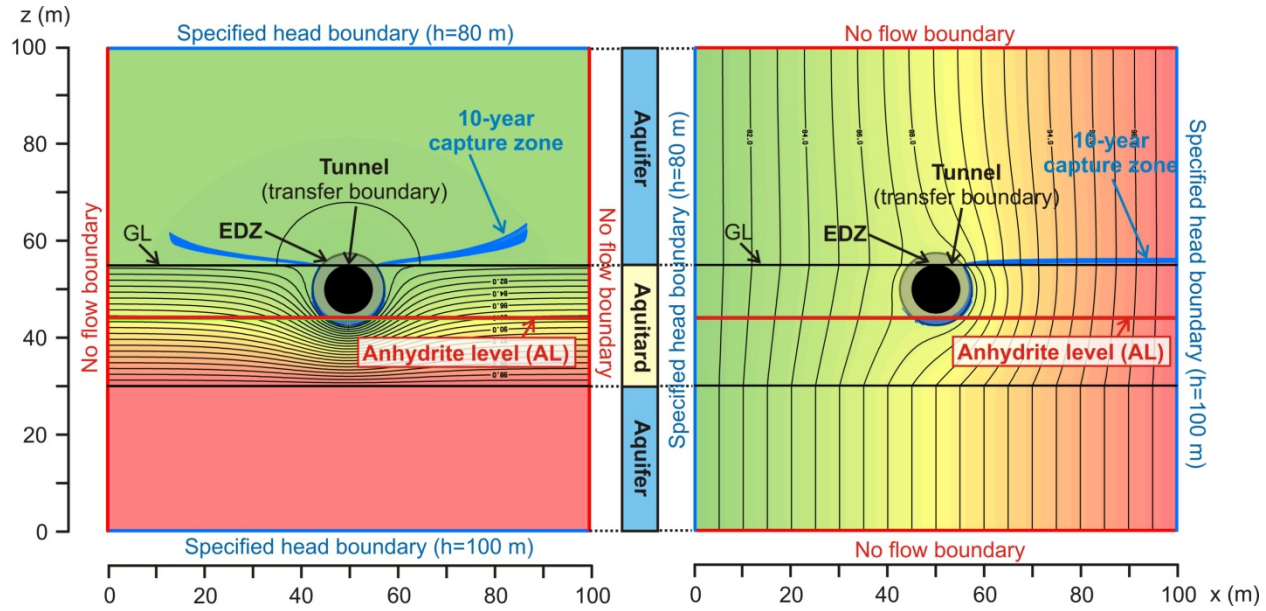

Figure 7: Influence of topographic position on hydraulic conditions after tunneling (contour lines of hydraulic head in black, 10-year capture zone in blue). The left figure corresponds to a "valley position" (c.f., Figure 2), the right figure corresponds to a "slope position". The reference model (Figure 6 right) corresponds to a "hill position". In all positions, water from the aquifer above the tunnel reaches the AL within (less than) 10 years, which can result in the transformation of anhydrite into gypsum and rock swelling.

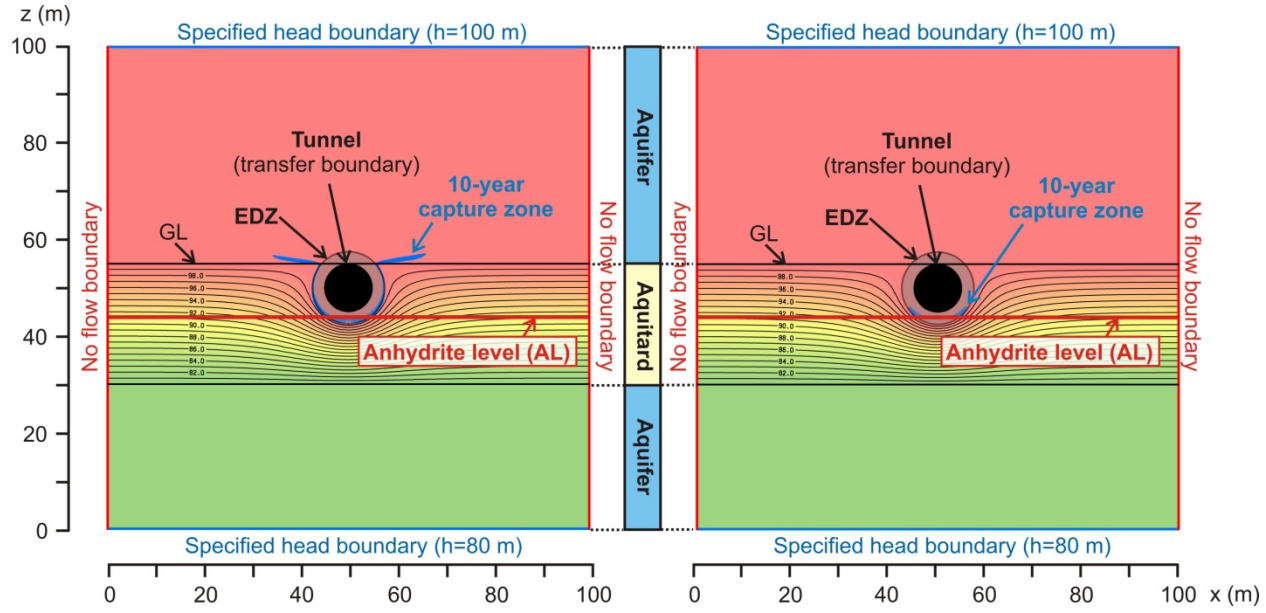

Figure 8: Influence of tunnel sealing on hydraulic conditions after tunneling (contour lines of hydraulic head in black, 10-year capture zone in blue). The left figure corresponds to an outflow transfer rate of 2.3E-10 s^{-1} at the tunnel boundary, the right figure corresponds to an outflow transfer rate of 2.3E-11 s^{-1}. The reference model (Figure 6 right) corresponds to an outflow transfer rate of 2.3E-9 s^{-1}. In the scenario with an outflow transfer rate of 2.3E-11 s^{-1} (right figure), water from the aquifer above the tunnel does not reach the AL within (less than) 10 years, preventing the transformation of anhydrite into gypsum and rock swelling.

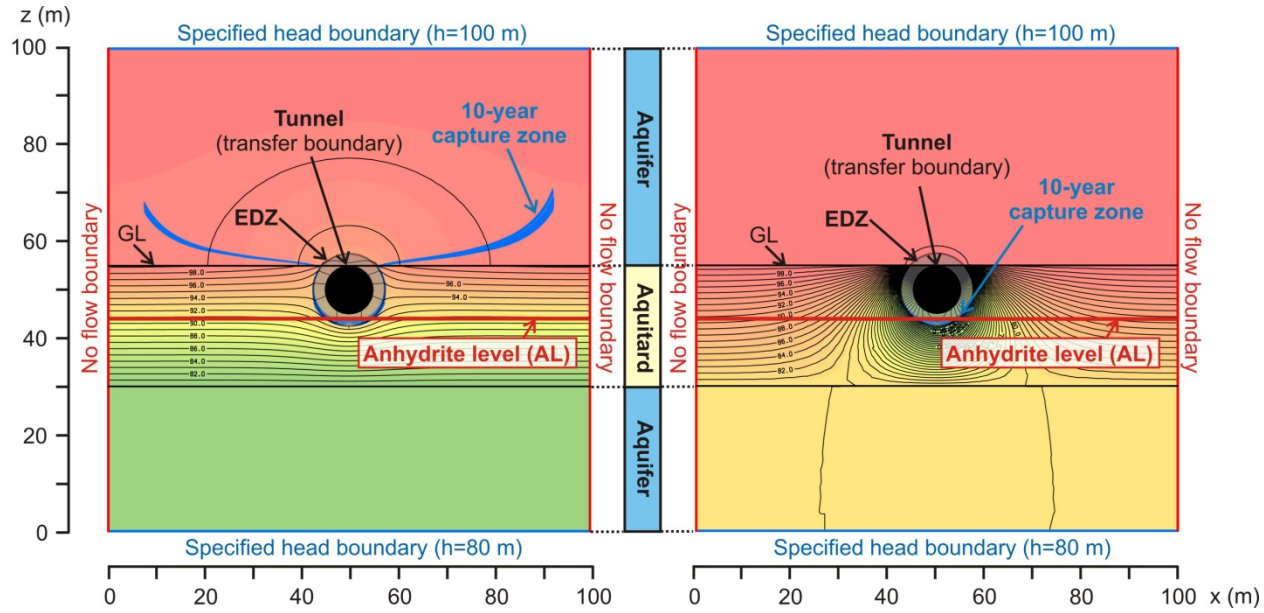

Figure 9: Influence of EDZ on hydraulic conditions after tunneling (contour lines of hydraulic head in black, 10-year capture zone in blue). The left figure corresponds to a hydraulic conductivity of 1.0E-6 ms^{-1} within the EDZ, the right figure corresponds to a hydraulic conductivity of 1.0E-8 ms^{-1}. The reference model (Figure 6 right) corresponds to a hydraulic conductivity of 1.0E-4 ms^{-1}. In the scenario with a hydraulic conductivity of 1.0E-8 ms^{-1} within the EDZ (right figure), water from the aquifer above the tunnel does not reach the AL within (less than) 10 years, preventing the transformation of anhydrite into gypsum and rock swelling.

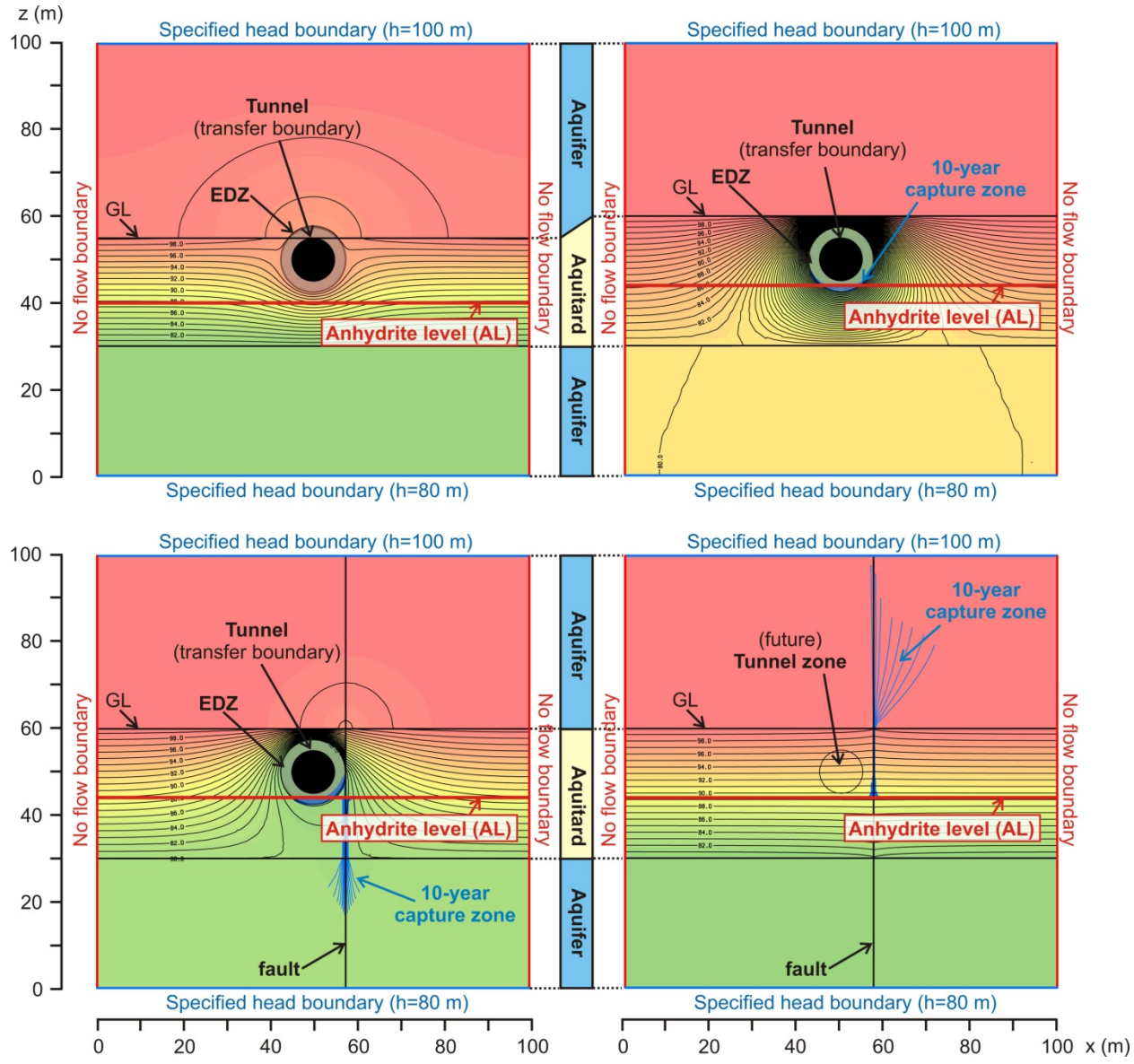

Figure 10: Influence of geological configuration on hydraulic conditions after tunneling (contour lines of hydraulic head in black, 10-year capture zone in blue). The top two figures correspond to a configuration where the anhydrite level (AL) is not linked to the aquifer above the tunnel by the EDZ (i.e., in the left figure, the AL is situated below (outside) the EDZ, in the right figure, the base of the aquifer above the tunnel is situated above (outside) the EDZ). In both cases, water from the aquifer above the tunnel does not reach the AL within (less than) 10 years, preventing the transformation of anhydrite into gypsum and rock swelling. The bottom two figures correspond to a situation, where a fault provides a link between an aquifer and the AL (left after tunneling, right before tunneling). The fault allows water access to the AL both before and after tunneling, which can result in the transformation of anhydrite into gypsum and rock swelling.

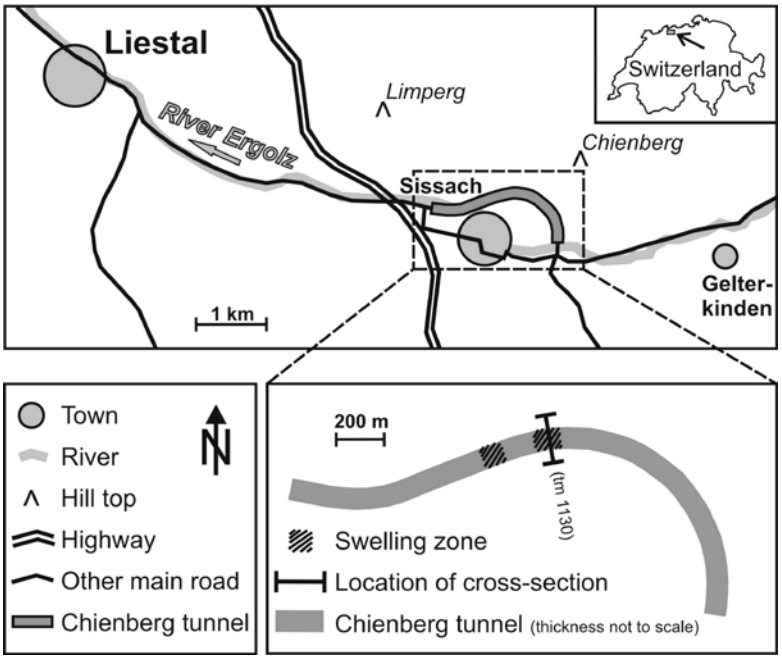

Figure 11: Location of study site.

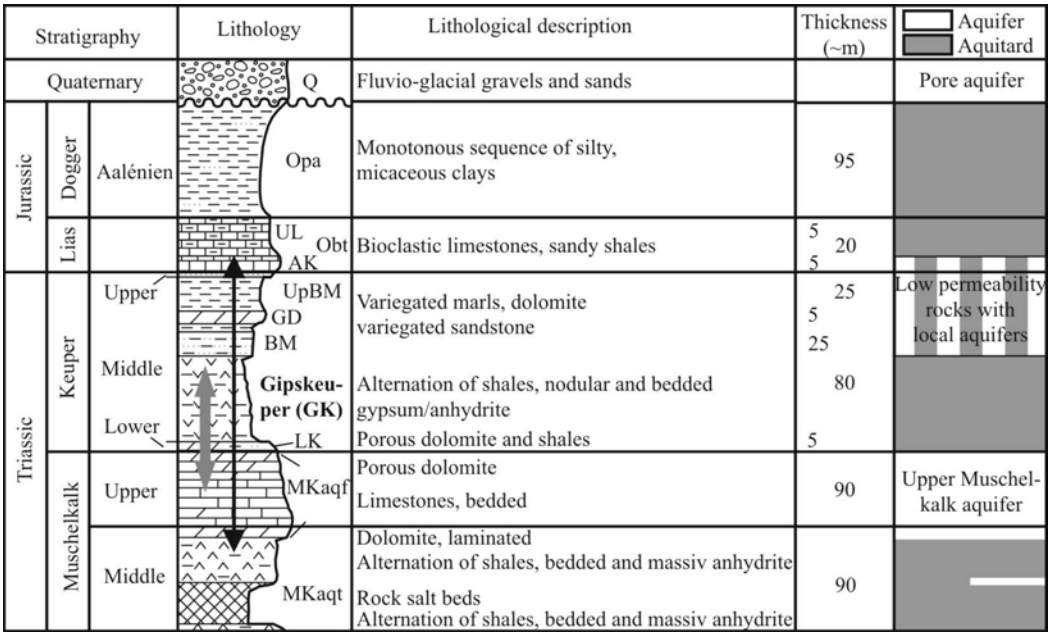

Figure 12: Schematic, stratigraphic section also showing hydrogeological characteristics of the study area (modified from Bitterli-Brunner and Fischer, 1988; Pearson et al., 1991). Grey arrow indicates stratigraphic extent of synthetic situations, black arrow of case study. Abbreviations of geological units: Q: Quaternary, Opa: Opalinus Clay, UL: Upper Lias, Obt: Obtusus Clay, AK: Arietenkalk, UpBM: Upper Bunte Mergel, GD: Gansinger Dolomite, BM: Bunte Mergel, GK: Gipskeuper, LK: Lettenkeuper, MKaqf: Muschelkalk aquifer, MKaqt: Muschelkalk aquitard.

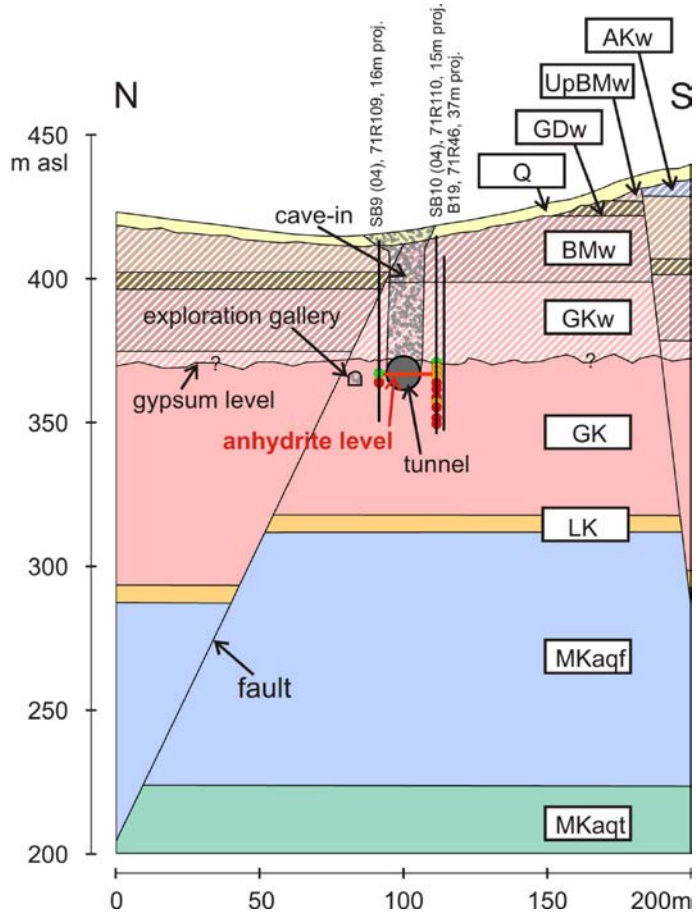

Figure 13: Cross-section of case study (abbreviations of geological units see Figure 12, "w" after geological unit indicates that this unit is weathered) [after *Butscher et al.*, 2011b]. Black lines indicate exploration drill holes. Dots indicate sulfate analysis samples (green: sulfate present as gypsum, red: sulfate present as anhydrite, orange: sulfate present as gypsum and anhydrite). Red line indicates anhydrite level. Dotted areas represent a cave-in area and a exploration gallery.

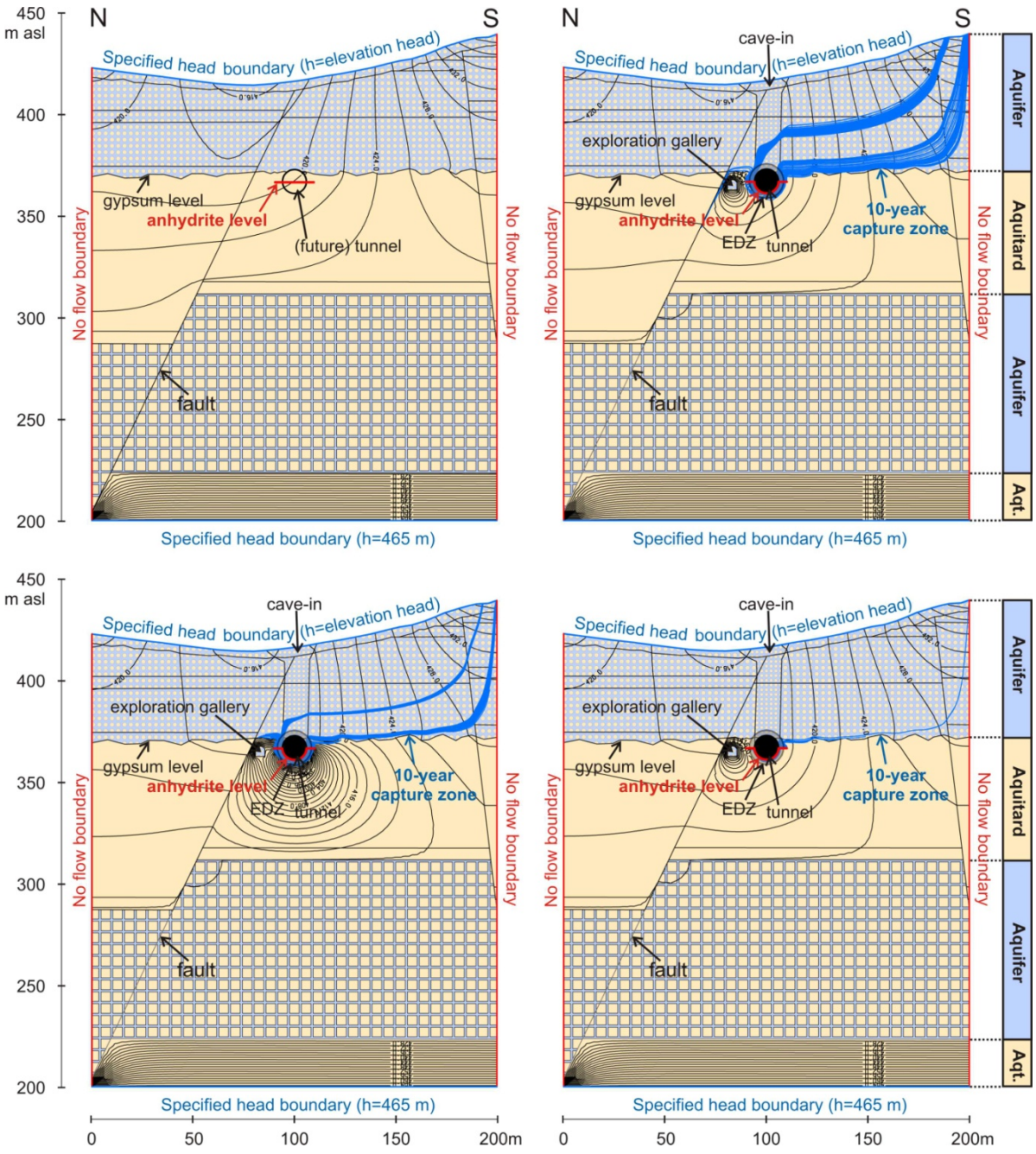

Figure 14: Hydraulic head field (black lines) and 10-year capture zone (blue lines) of the anhydrite level (red bar) calculated with the groundwater model of the case study. Top left: conditions before tunneling (the 10-year capture zone is too short to be displayed). Top right: Conditions after tunneling assuming a hydraulic conductivity of 1.0E-4 ms^{-1} in the EDZ and an outflow transfer rate of 2.3E-9 s^{-1} at the tunnel boundary (the values correspond to the reference model of chapter 4). Bottom left: Corresponds to figure top right, but hydraulic conductivity in EDZ is decreased by a factor of 10,000 to 1.0E-8 ms^{-1}. Bottom right: Corresponds to figure top right, but outflow transfer rate at tunnel boundary is decreased by a factor of 100 to 2.3E-11 s^{-1}, representing the sealing effect of the tunnel liner. In all scenarios, water from the aquifer above the tunnel reaches the AL within (less than) 10 years after tunneling, which can result in the transformation of anhydrite into gypsum and rock swelling. In the sceanrios with a decreased hydraulic conductivity of the EDZ and decrease outflow transfer rate at the tunnel boundary (bottom row), the 10-year capture zone is narrower than in the reference situation (top right), indicating reduced water access to the AL which can result in reduced transformation of anhydrite into gypsum and reduced rock swelling.